

Bridging the Gap: Transitioning
from Deterministic to
Stochastic Interaction Modeling
in Electrochemistry

Phase-Field Modeling of Microstructural Evolution Resulting from Corrosion

Katsuyo Thornton
University of Michigan

Acknowledgments



Funding: Molten Salt in Extreme Environment (MSEE) EFRC
Center for PRedictive Integrated Structural Materials Science (PRISMS)
Computational Resources: NSF XSEDE/ACCESS, DOE NERSC, UM ARC

Students & Postdocs (*Alumni):



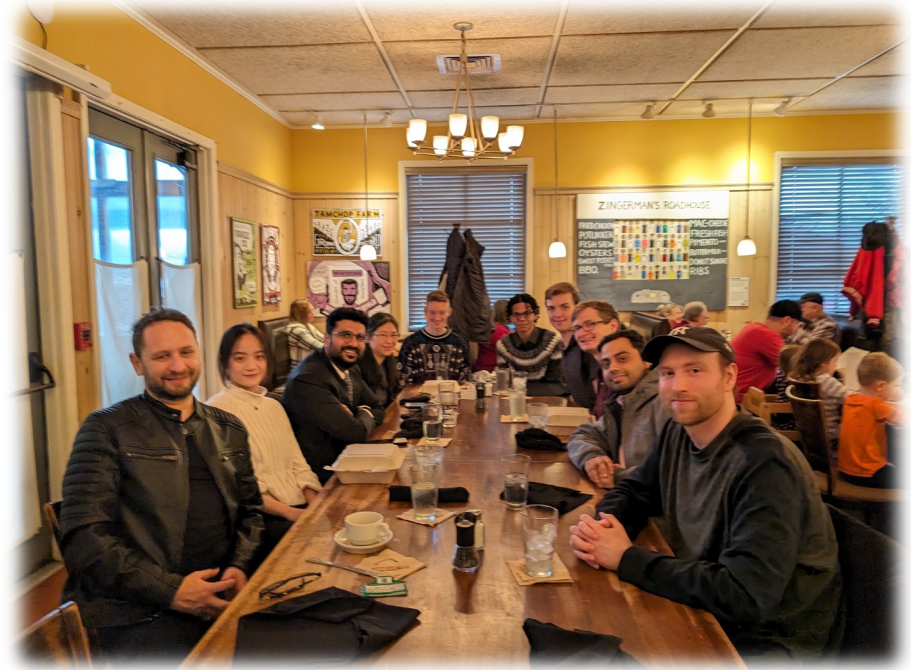
Advancing
Innovation



Beck Andrews, Vishwas Goel (industry)*,
Ellery Hendrix, Steve DeWitt (ORNL)*, and
Alex Chadwick (NRL)*

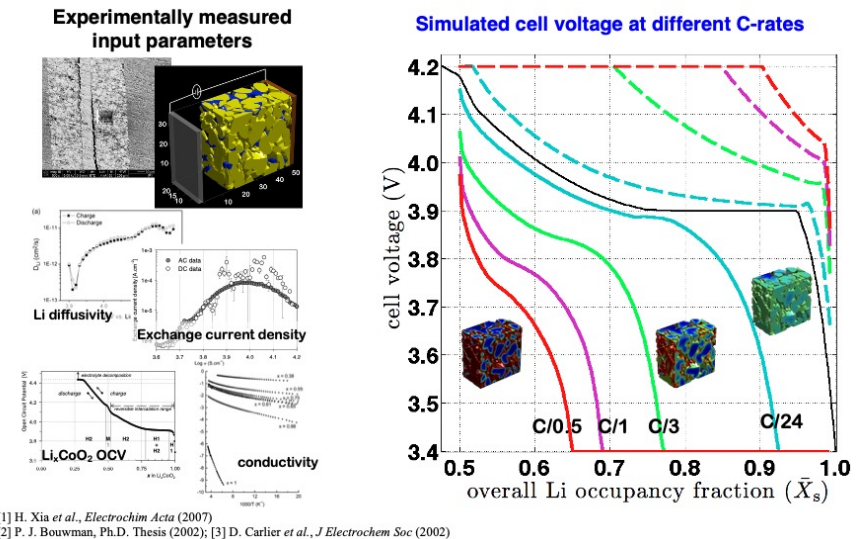
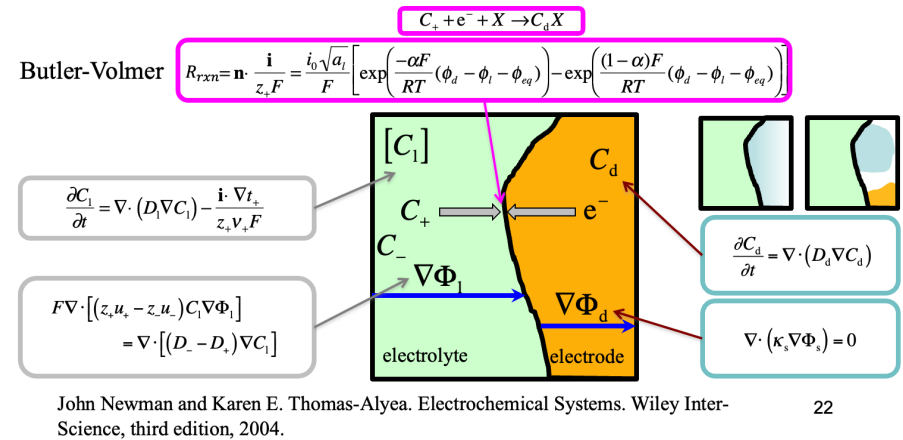


Collaborators: David Montiel (PRISMS),
Karen Chen-Wiegart (Stony Brook/BNL)



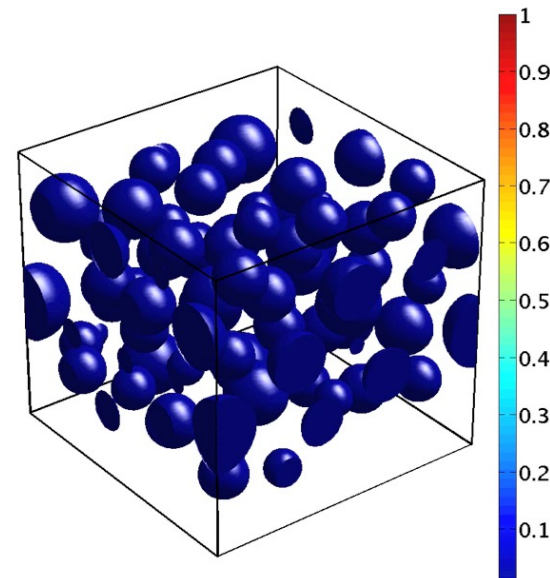
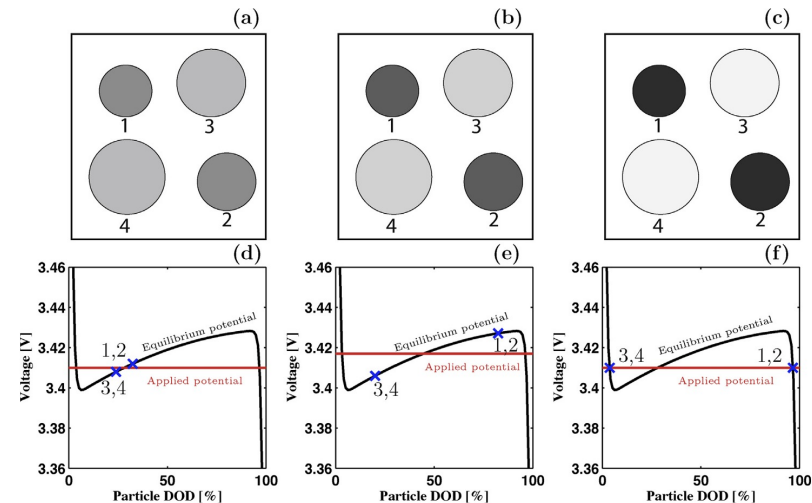
Thornton IPAM Talks So Far

- Tutorial 1: The Role of Materials and Microstructures in Electrochemical Energy Storage Part 1
- Tutorial 2: The Role of Materials and Microstructures in Electrochemical Energy Storage Part 1
- Hands-On Session
- Today: Corrosion & Microstructural Evolution



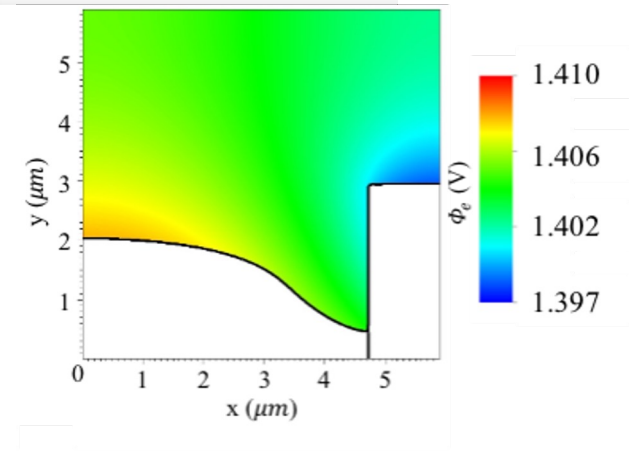
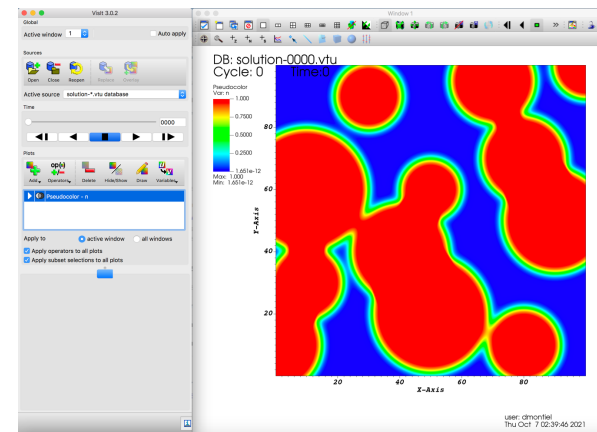
Thornton IPAM Talks So Far

- Tutorial 1: The Role of Materials and Microstructures in Electrochemical Energy Storage Part 1
- Tutorial 2: The Role of Materials and Microstructures in Electrochemical Energy Storage Part 1
- Hands-On Session
- Today: Corrosion & Microstructural Evolution



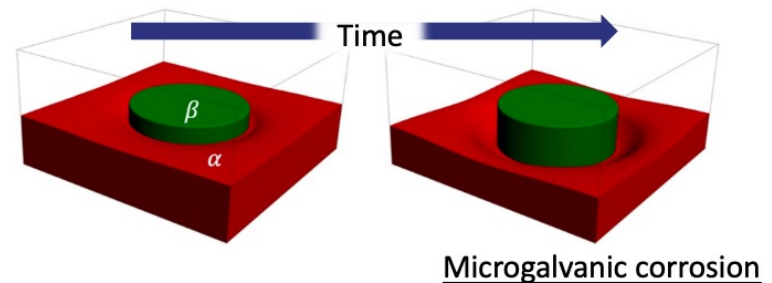
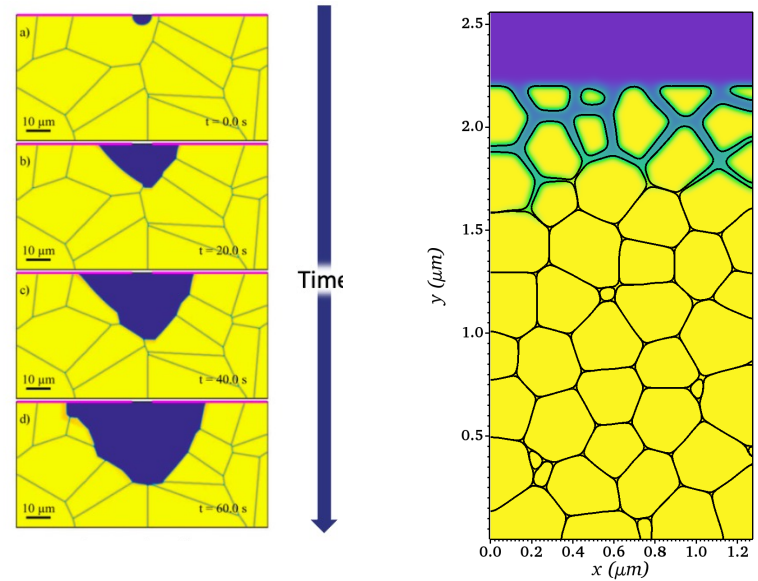
Thornton IPAM Talks So Far

- Tutorial 1: The Role of Materials and Microstructures in Electrochemical Energy Storage Part 1
- Tutorial 2: The Role of Materials and Microstructures in Electrochemical Energy Storage Part 1
- Hands-On Session
- Today: Corrosion & Microstructural Evolution

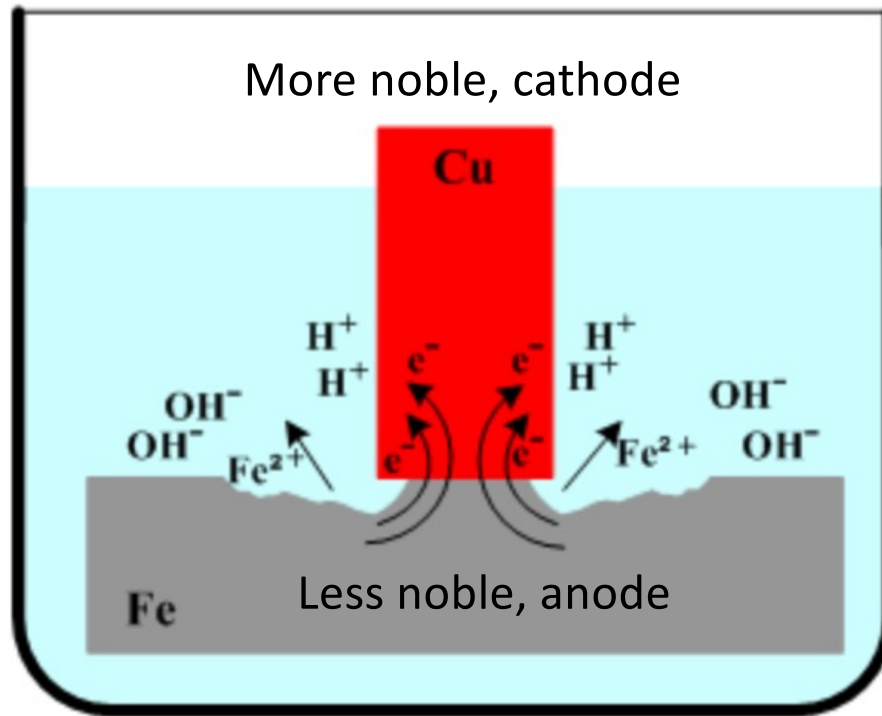


Thornton IPAM Talks So Far

- Tutorial 1: The Role of Materials and Microstructures in Electrochemical Energy Storage Part 1
- Tutorial 2: The Role of Materials and Microstructures in Electrochemical Energy Storage Part 1
- Hands-On Session
- Today: Corrosion & Microstructural Evolution

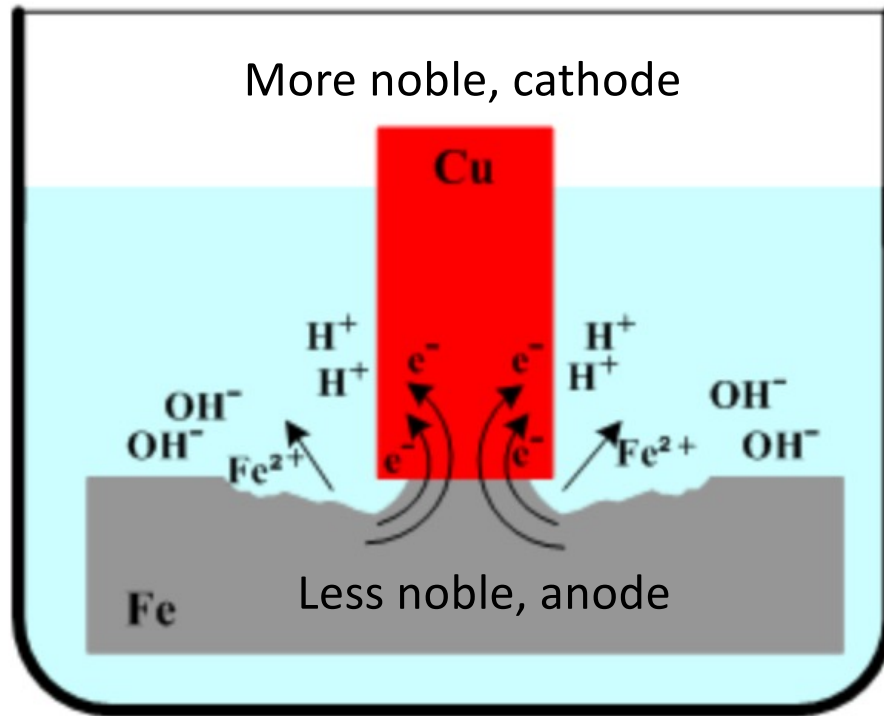


What is Galvanic Corrosion?



www.substech.com

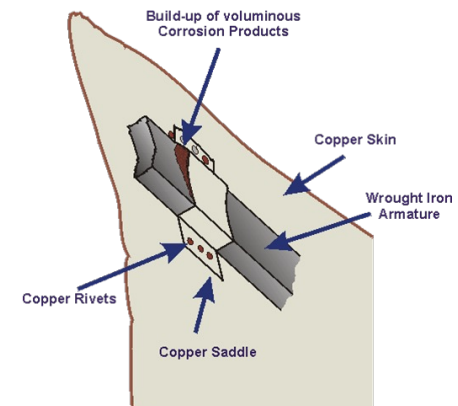
What is Galvanic Corrosion?



www.substech.com

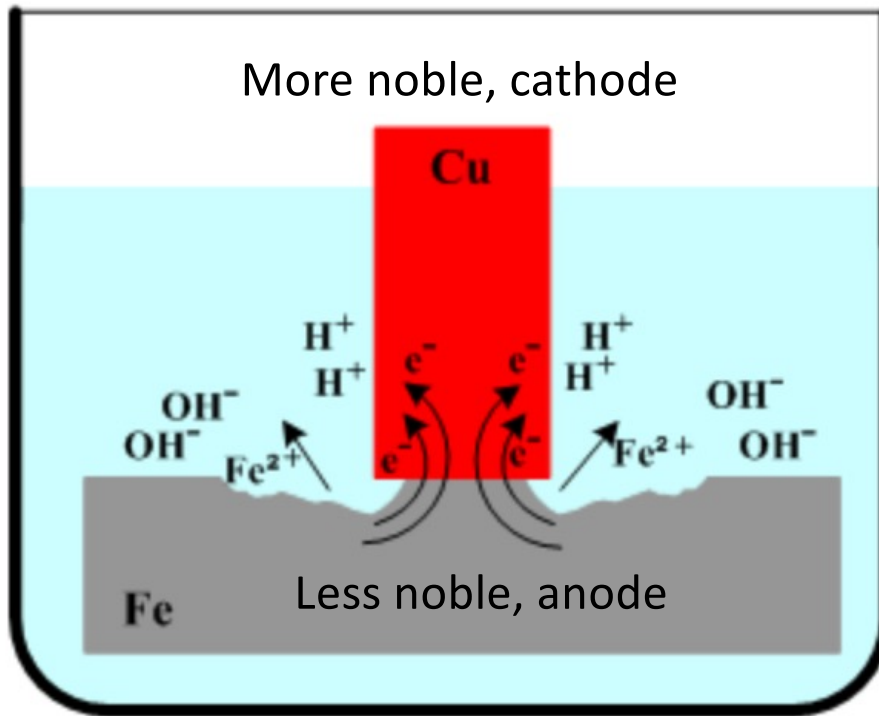


Source: Public domain



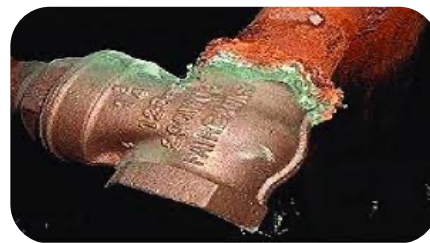
Source: Public domain

What is Galvanic Corrosion?

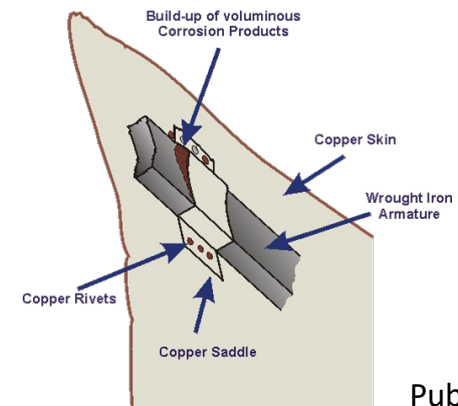


Public domain

www.substech.com



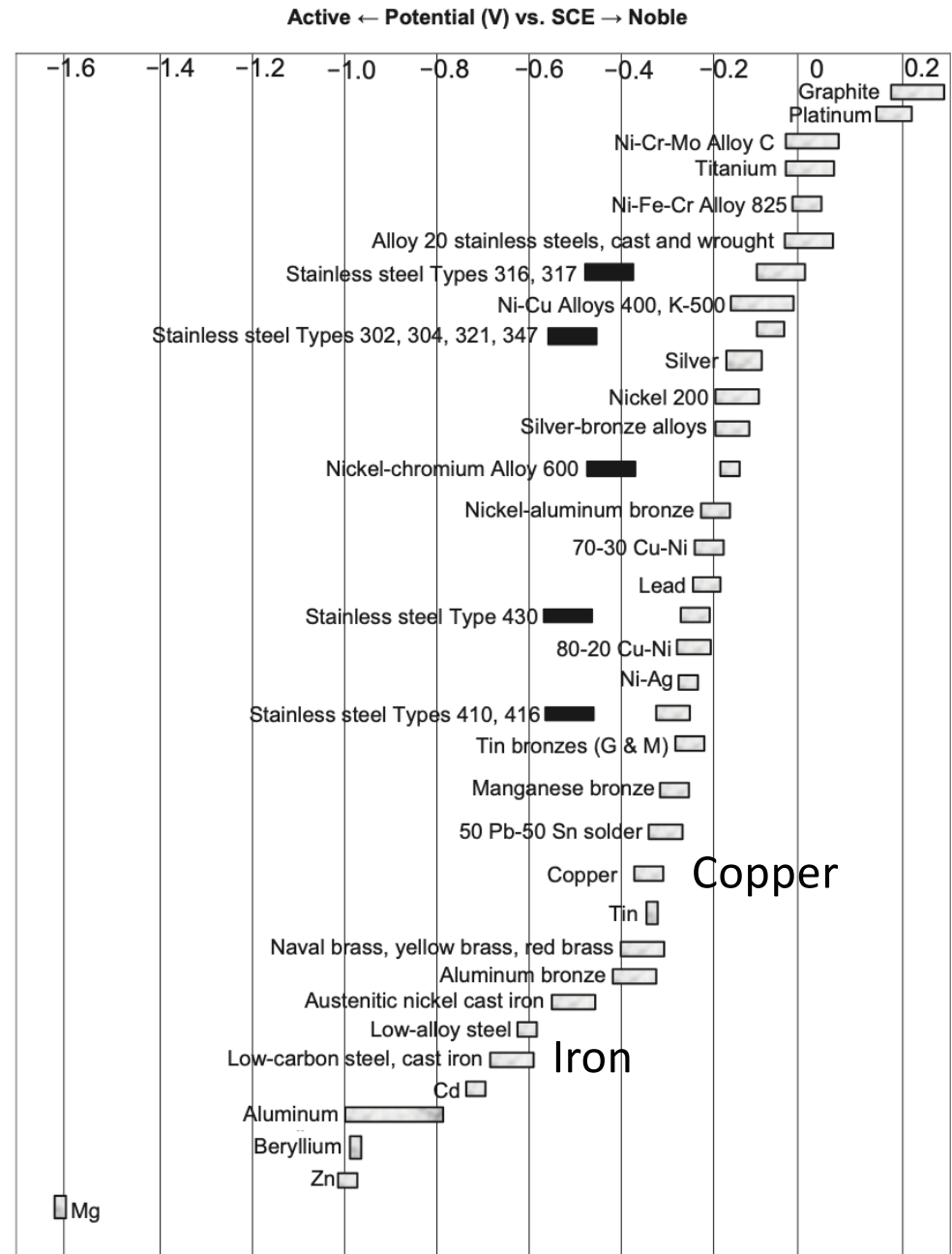
Palanisamy, DOI: 10.5772/intechopen.80542



Public domain

Galvanic Series

H.P. Hack, Evaluating galvanic corrosion, in: Corrosion: Fundamentals, Testing and Protection, 9th ed., vol. 13A, ASM Handbook, Metals Park, OH, 1987, pp. 562–567.



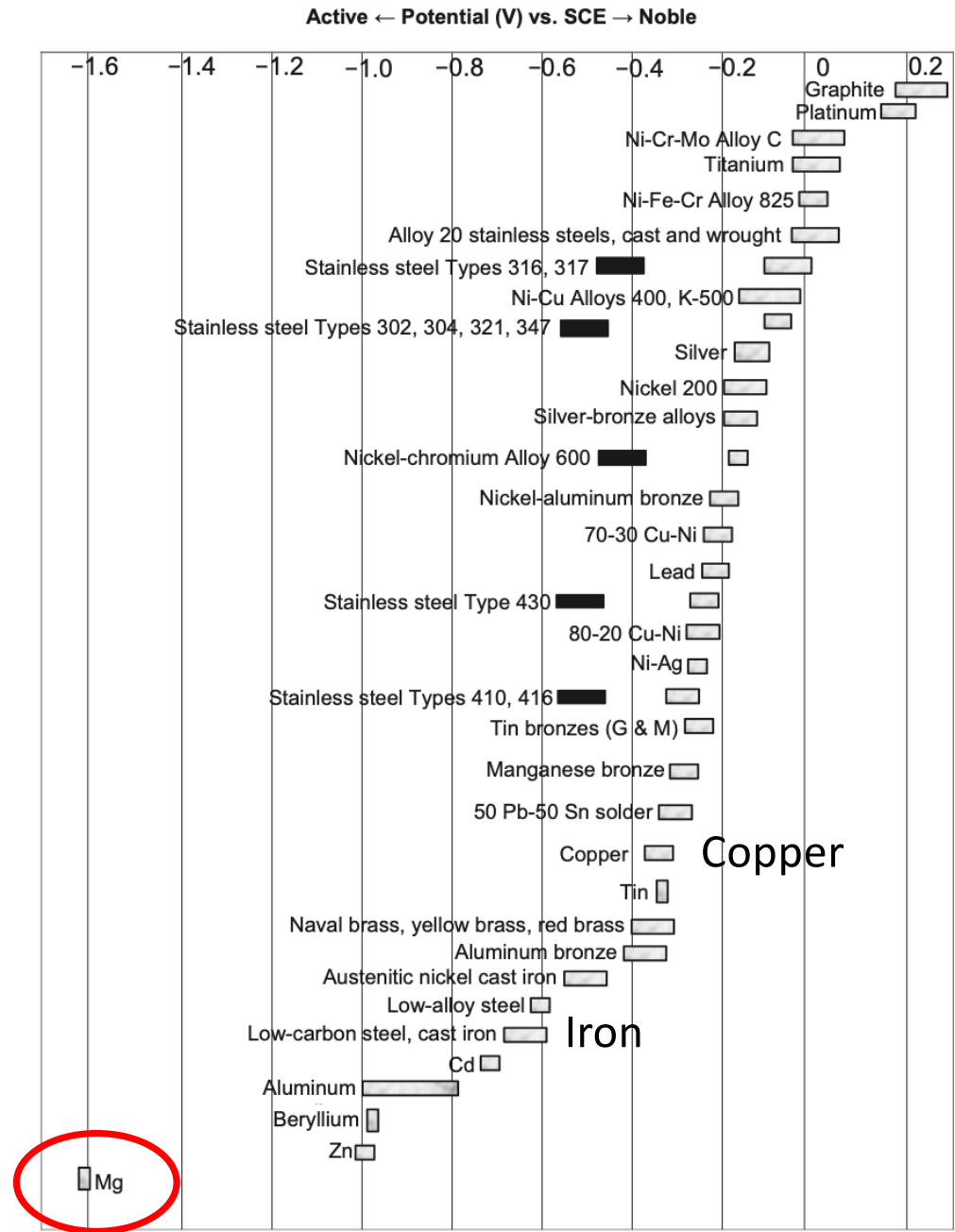
Galvanic Series

H.P. Hack, Evaluating galvanic corrosion, in: Corrosion: Fundamentals, Testing and Protection, 9th ed., vol. 13A, ASM Handbook, Metals Park, OH, 1987, pp. 562–567.

PRISMS Center focuses on advancing magnesium alloys as lightweight structural materials

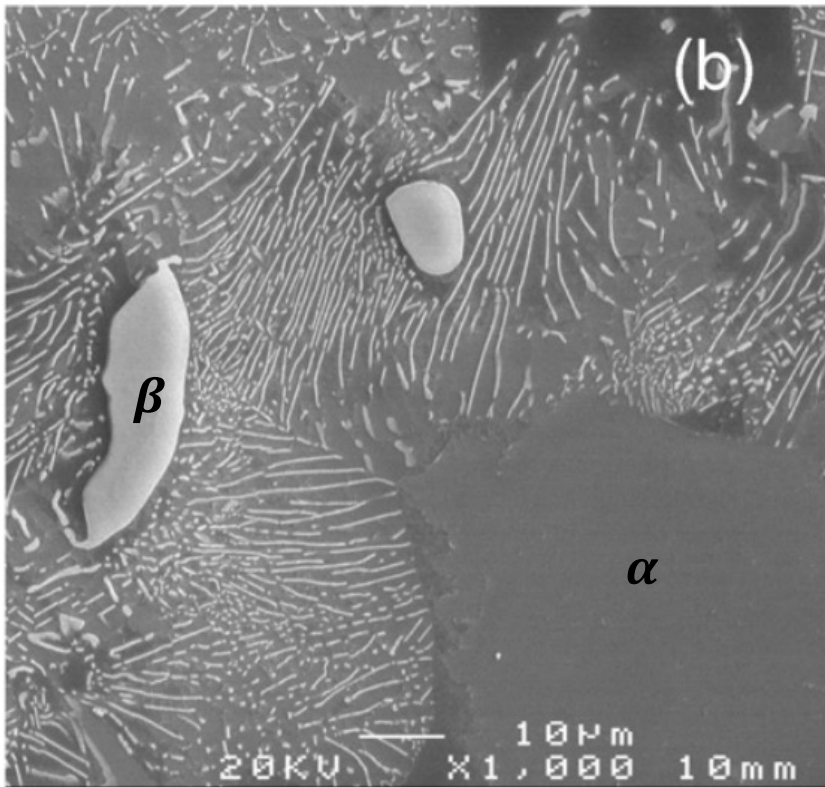
Improved mechanical properties can be achieved via alloying

Magnesium



Microgalvanic Corrosion

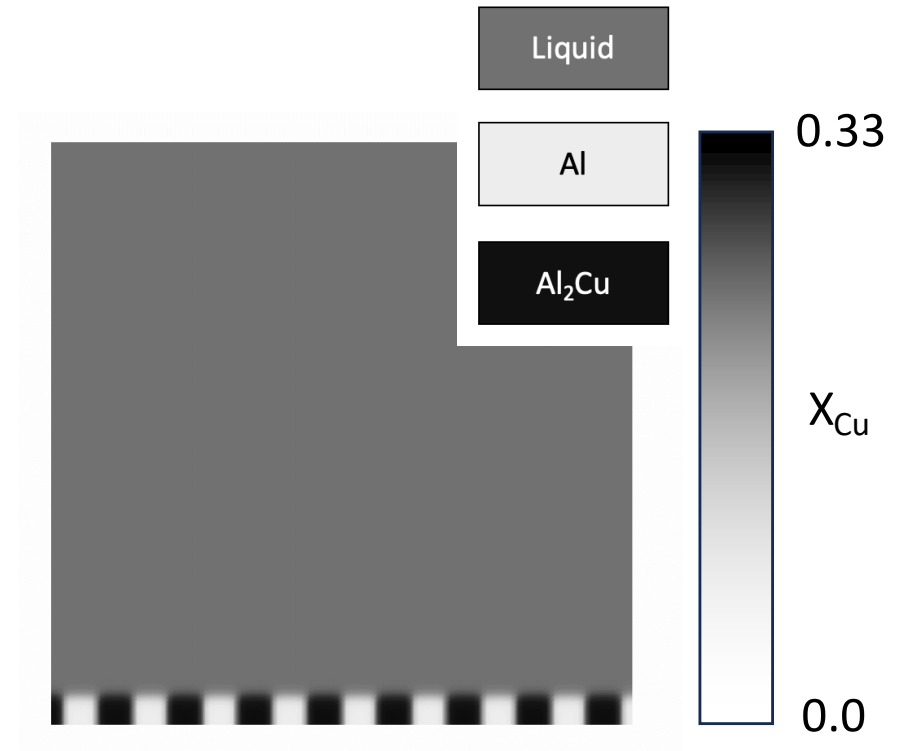
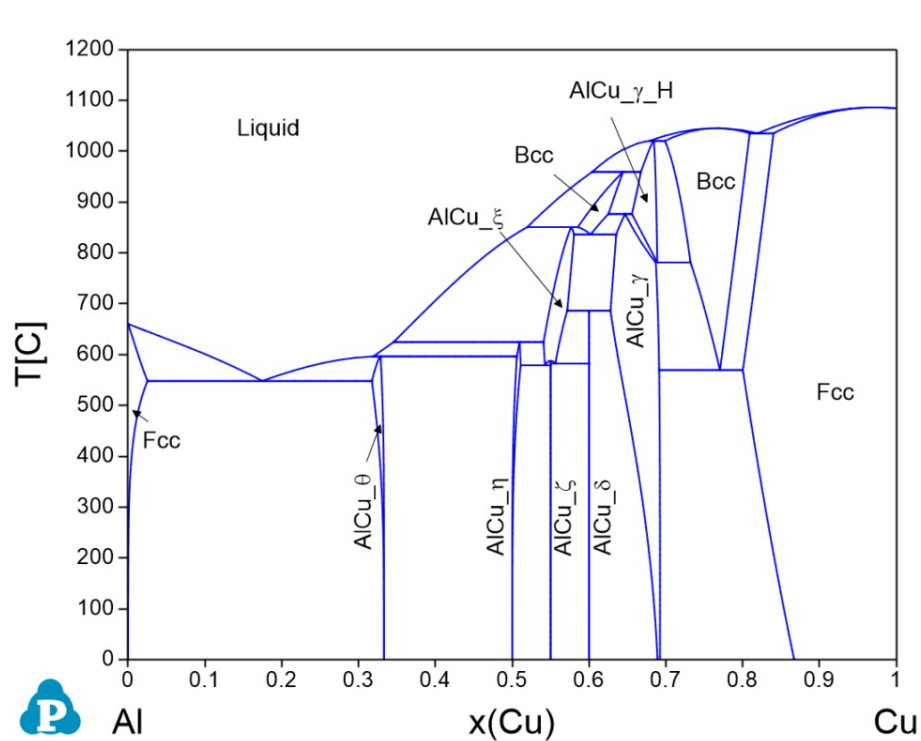
As-cast magnesium alloy (AZ91)



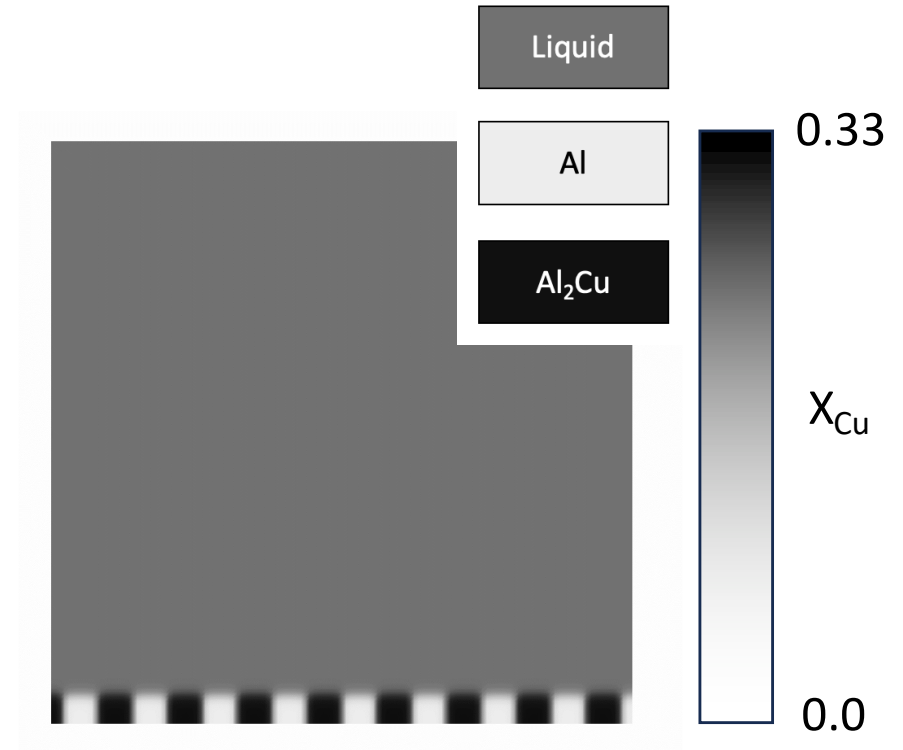
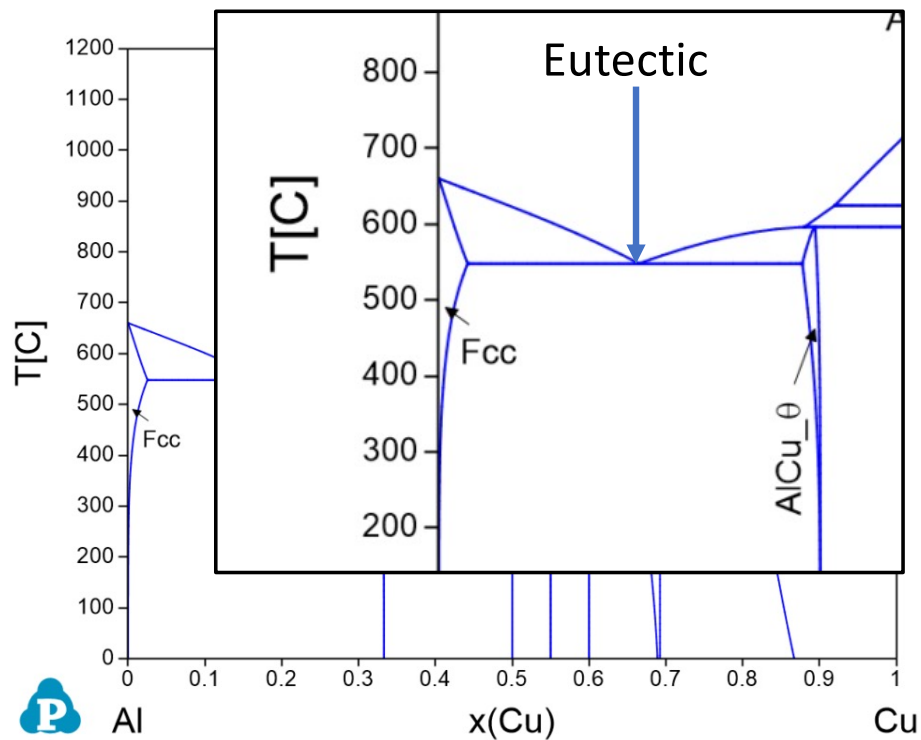
The presence of multiple phases (regions with different concentrations) causes a galvanic effect!

Zhao et al., Corrosion Science 50 (2008) 1939–1953

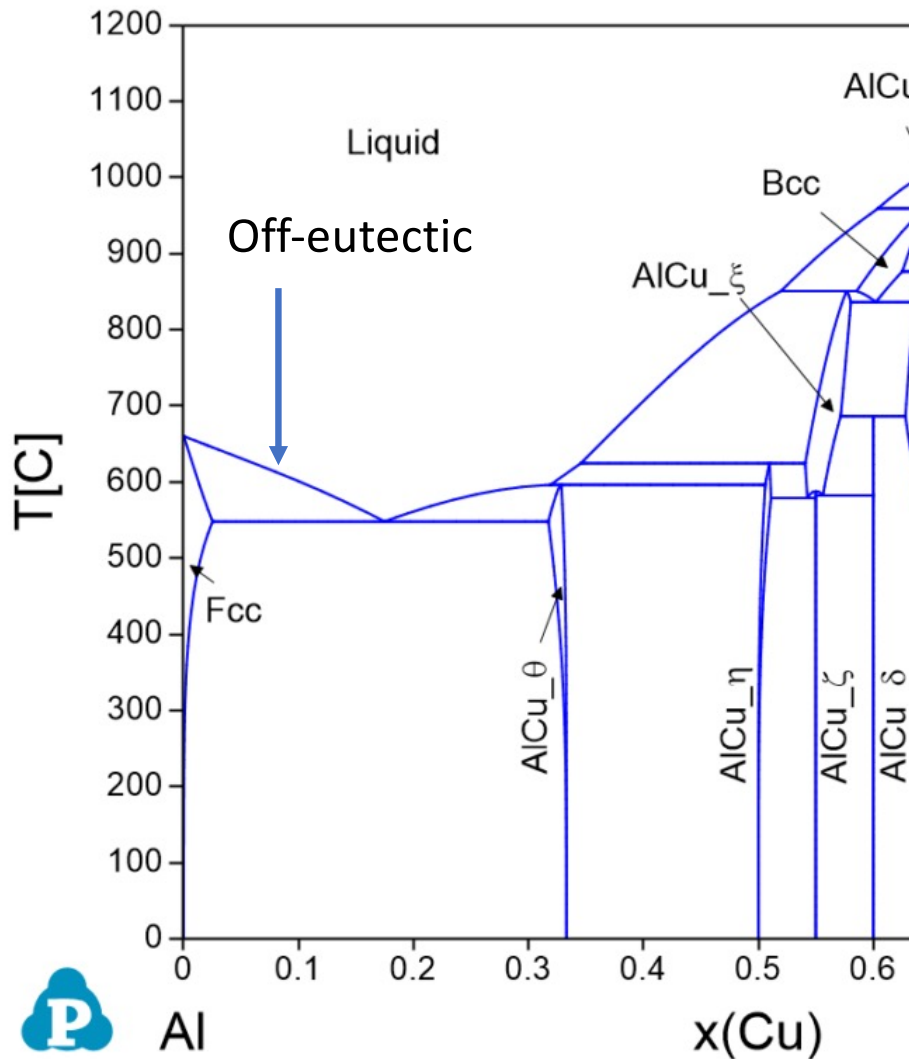
Microstructure Example: Eutectic Solidification



Microstructure Example: Eutectic Solidification



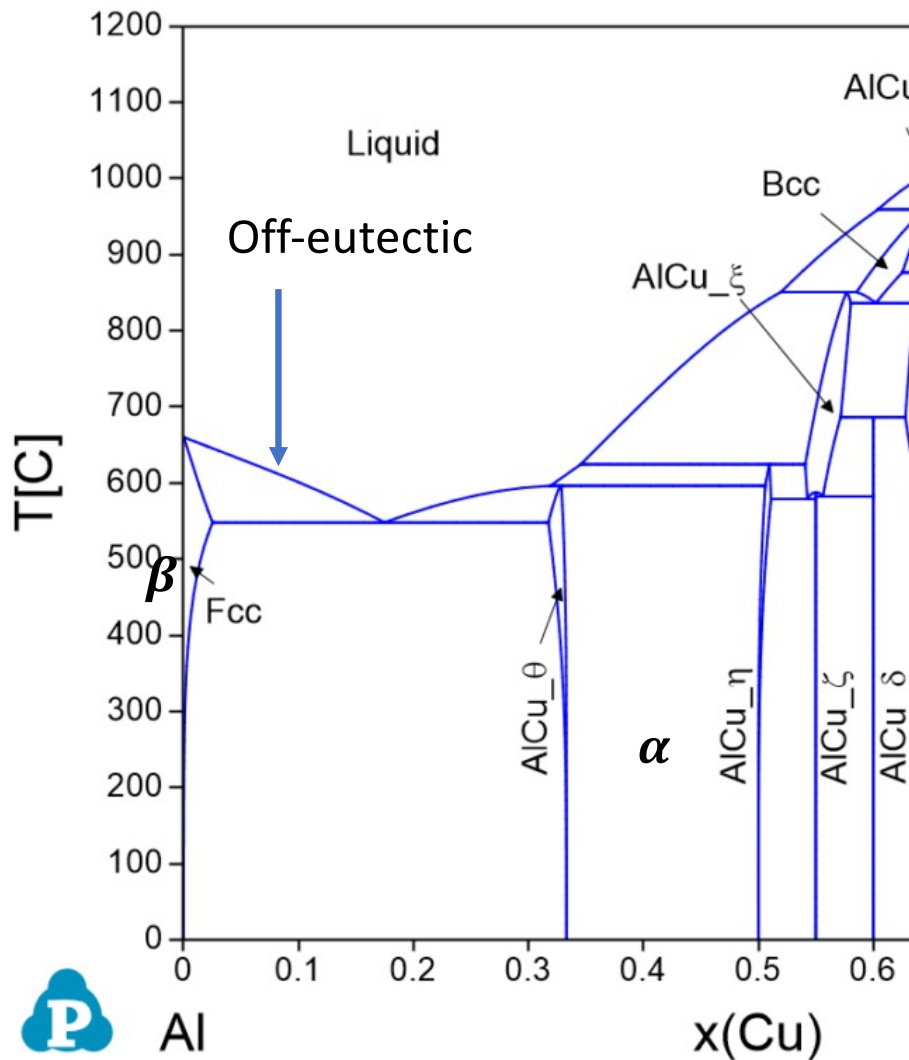
Microstructure Example: Eutectic Solidification



- Formation of “primary”
- Enrichment of Cu in liquid
- Primary grow
- Liquid concentration hits the eutectic value
- Eutectic microstructure forms around the primary

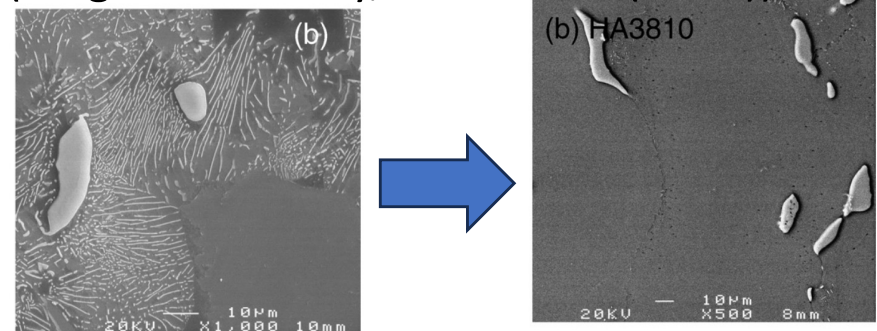


Microstructure Example: Eutectic Solidification



- Formation of “primary”
- Enrichment of Cu in liquid
- Primary grow
- Liquid concentration hits the eutectic value
- Eutectic microstructure forms around the primary
- Subsequent **heat treatment** can alter the microstructure

(magnesium alloy, Zhao et al. (2008))



Phase-Field Model for Localized Corrosion with the Smoothed Boundary Method

Kinetics at the interface: reaction current

$$\frac{i_{rxn}}{i_{corr}} = \left(1 - \frac{i_{rxn}}{i_{max,c}}\right) \exp\left(\frac{z_M(1-\beta)F}{RT}\eta\right)$$

$$\eta = V_s - E_{corr} - \Phi$$

Evolution of phases in the metal (grains or intermetallic particles)

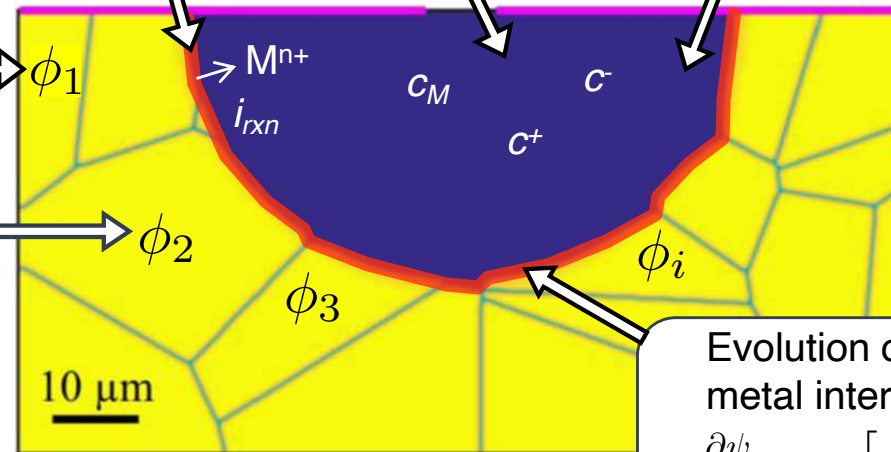
$$\frac{\partial \phi_i}{\partial t} = \nabla \cdot \left[M(\psi) \nabla \frac{\delta \mathcal{F}}{\delta \phi_i} \right] - \frac{V_M i_{rxn}}{z_M F} |\nabla \psi|$$

Ionic transport within the electrolyte (smooth boundary method)

$$\frac{\partial c_i}{\partial t} = \frac{1}{\psi} \nabla \cdot (\psi D_i \nabla c_i) + \frac{1}{\psi} \left(\frac{z_i F}{RT} \nabla \cdot (\psi D_i c_i \nabla \Phi) \right) + \frac{|\nabla \psi|}{\psi} \left(\frac{i_{rxn}}{z_i F} \right)$$

Electrostatic potential

$$\nabla \cdot (\psi \kappa \nabla \Phi) = F \nabla \cdot \left(\psi \sum_{j=1}^{n-1} z_j (D_n - D_j) \nabla c_j \right) - |\nabla \psi| i_{rxn}$$



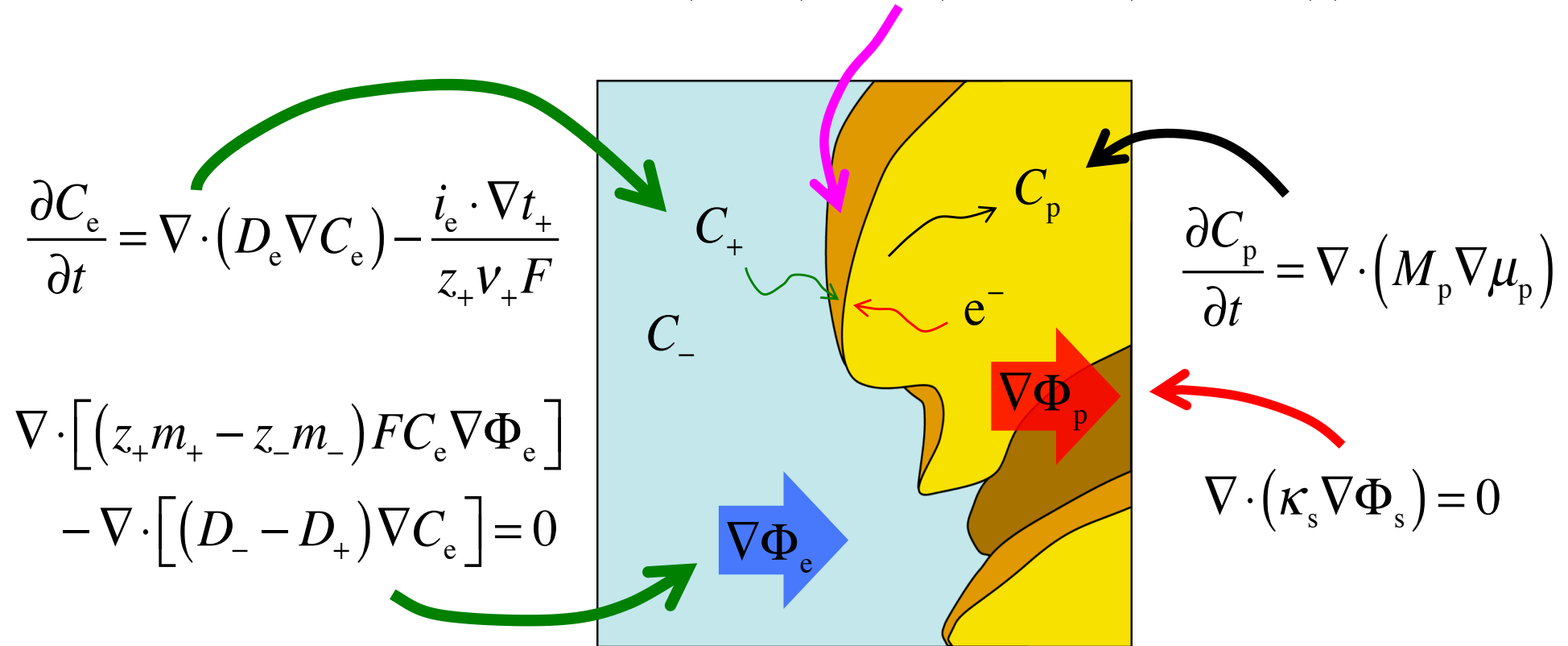
Evolution of the electrolyte-metal interface

$$\frac{\partial \psi}{\partial t} = \nabla \cdot \left[M(\psi) \nabla \frac{\delta \mathcal{F}}{\delta \psi} \right] + \frac{V_M i_{rxn}}{z_M F} |\nabla \psi|$$

A. Chadwick, J. Stewart, R. A. Enrique, S. Du, and K. Thornton, *J. Electrochem. Soc.*, 165 (10) C633 (2018).

Similarities to Microscale Model of Battery Lithiation/Delithiation

$$i_0(C_p^{surf}, C_e) \left(\exp\left(\frac{0.5F}{RT}\eta\right) - \exp\left(\frac{-0.5F}{RT}\eta\right) \right)$$



Ref: Doyle et al., Journal of the Electrochemical Society, 140, 6, 1993

Pit Growth within a Single Grain

Chadwick, et al.

- Exposed metal surface (top)

$V_s = 50 \text{ mV}$; $E_{\text{corr}} = -0.24 \text{ vs SCE}$, $i_{\text{corr}} = 0.99 \text{ mA/cm}^2$

- Boundary conditions are uniform throughout the top of the domain

$c_M = 0 \text{ M}$, $c_+ = 1 \text{ M}$, and $\Phi = 0 \text{ V vs. SCE}$

- Motion of the electrolyte/single metal grain interface is tracked

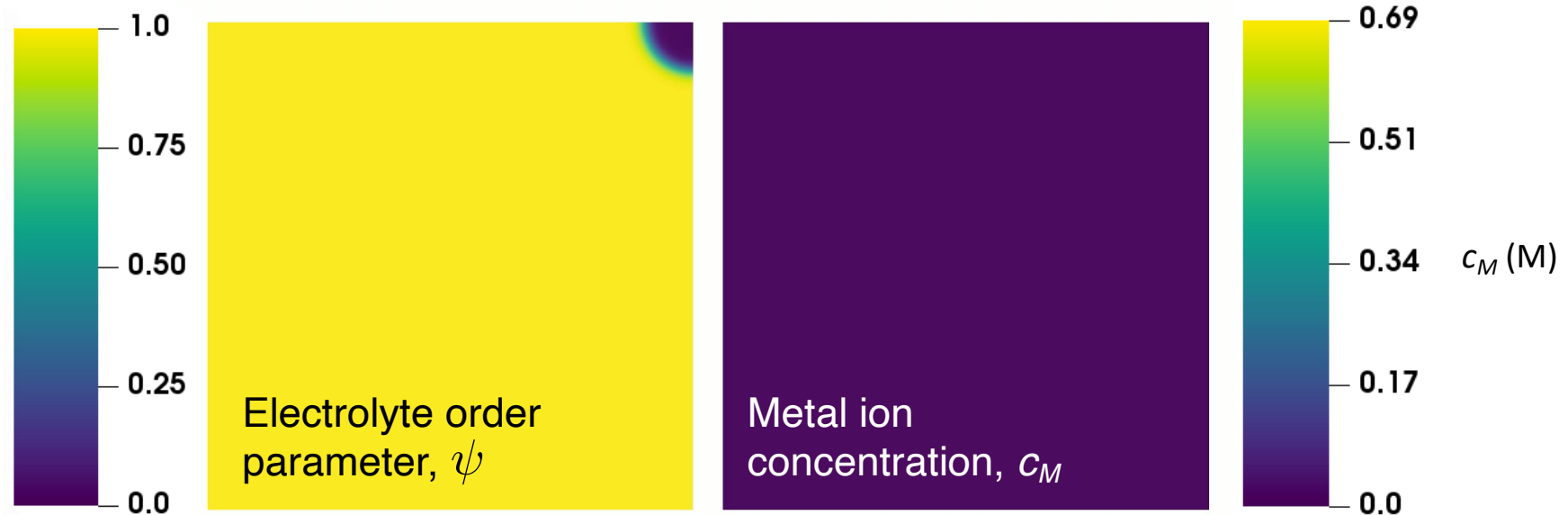
$$\nabla \cdot (\psi \kappa \nabla \Phi) = F \nabla \cdot \left(\psi \sum_{j=1}^{n-1} z_j (D_n - D_j) \nabla c_j \right) - |\nabla \psi| i_{\text{rxn}}$$

$$\frac{i_{\text{rxn}}}{i_{\text{corr}}} = \left(1 - \frac{c_M}{c_{M,\text{sat}}} \right) \exp \left(\frac{z_M (1 - \beta) F}{RT} \eta \right)$$

$$\eta = V_s - E_{\text{corr}} - \Phi$$

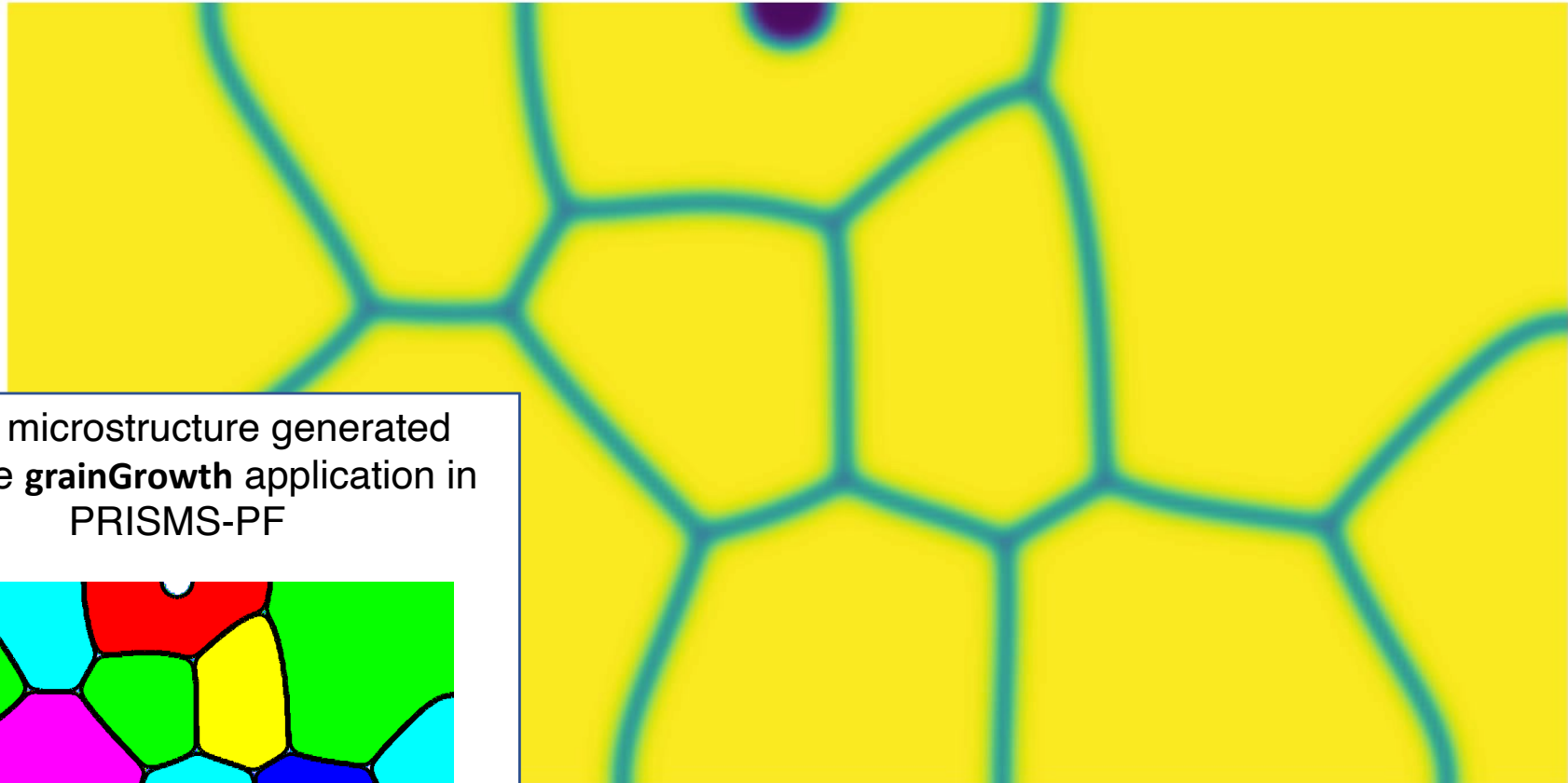
system size = $18.75 \mu\text{m} \times 18.75 \mu\text{m}$

time = 4 s

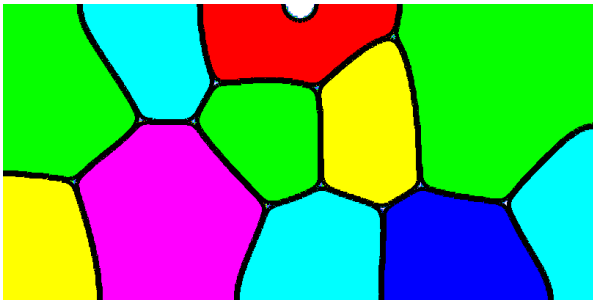


Pit Growth into a Polycrystal

Chadwick, et al.



Initial microstructure generated
with the **grainGrowth** application in
PRISMS-PF

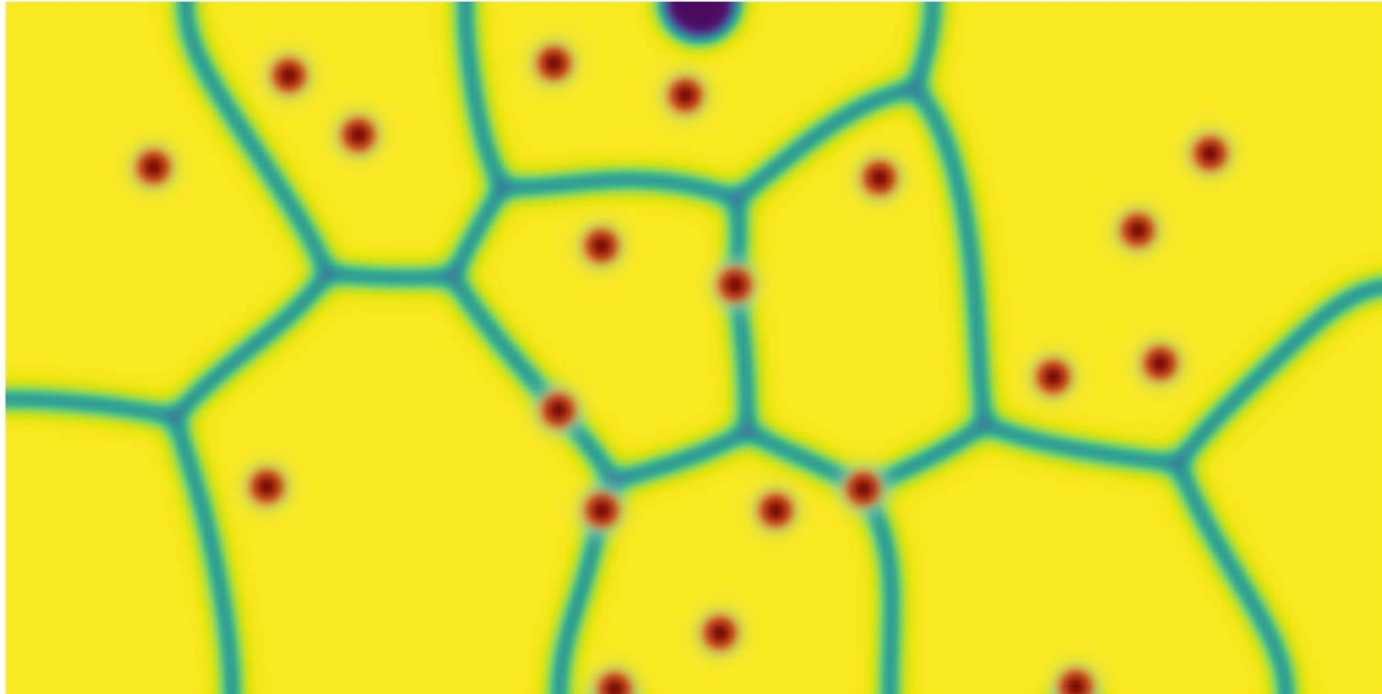


Polycrystal with Precipitates

Chadwick, et al.

$$\frac{i_{rxn}}{i_{corr}} = \left(1 - \frac{c_M}{c_{M,sat}}\right) \exp\left(\frac{z_M(1-\beta)F}{RT}\eta\right)$$

$$i_{corr,prec} = 5 \times i_{corr,matrix}$$



PRISMS-PF: An Open-Source Parallel Phase-Field Modeling Framework

prisms-center.github.io/phaseField

DeWitt et al., npj Comput. Mater. 6, 29 (2020)

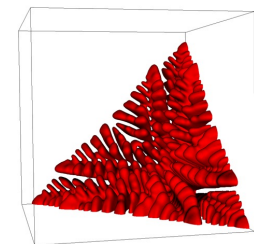
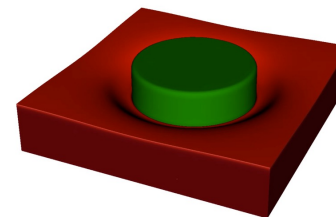
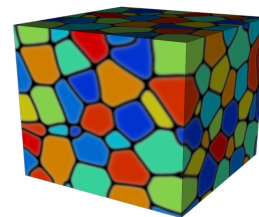
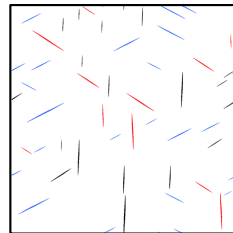
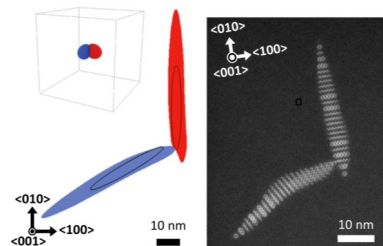


Advanced capabilities

- Based on the deal.II finite element library
- Matrix-free finite element approach
- Solution of an arbitrary number of coupled PDEs
- Up to 6th order elements
- Multi-level parallelism
- Adaptive meshing
- Explicit nucleus placement
- Grain-remapping
- Newton/Picard nonlinear solver

Functionalities / Ease of Use

- Simple interface
- Detailed online user guide
- 30 pre-built applications
- Simple Docker-based installation
- nanoHUB tool w/ GUI for educational use
- Integrated with Materials Commons
- Postprocessing scripts for results analysis
- YouTube video tutorials
- Virtual Machine
- Troubleshooting/FAQ page



COLLEGE OF ENGINEERING
MATERIALS SCIENCE & ENGINEERING
UNIVERSITY OF MICHIGAN



U.S. DEPARTMENT OF
ENERGY



MSEE
molten salts in extreme environments



PRISMS-PF Application to Mg Corrosion

MRS Communications (2022) 12:1050–1059

© The Author(s) 2022

<https://doi.org/10.1557/s43579-022-00266-6>



Computational Approaches for Materials Discovery
and Development Prospective



Simulating microgalvanic corrosion in alloys using the PRISMS phase-field framework

Vishwas Goel, Yanjun Lyu, Stephen DeWitt, David Montiel, Katsuyo Thornton^{id}, Department of Materials Science and Engineering, University of Michigan, Ann Arbor, MI 48150, USA

Address all correspondence to Katsuyo Thornton at ktthorn@umich.edu

(Received 6 May 2022; accepted 2 September 2022; published online: 17 October 2022)

Journal of The Electrochemical Society, 2023 **170** 101502



Understanding the Effect of Electrochemical Properties and Microstructure on the Microgalvanic Corrosion of Mg Alloys via Phase-Field Simulations

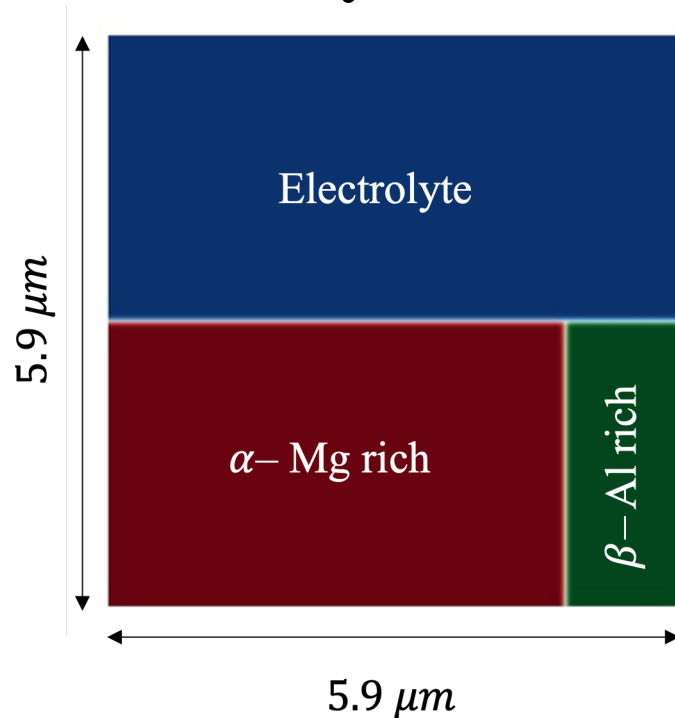
Vishwas Goel^{id}, **David Montiel**^{id}, and **Katsuyo Thornton**^{z id}

Department of Materials Science and Engineering, University of Michigan, Ann Arbor, United States of America

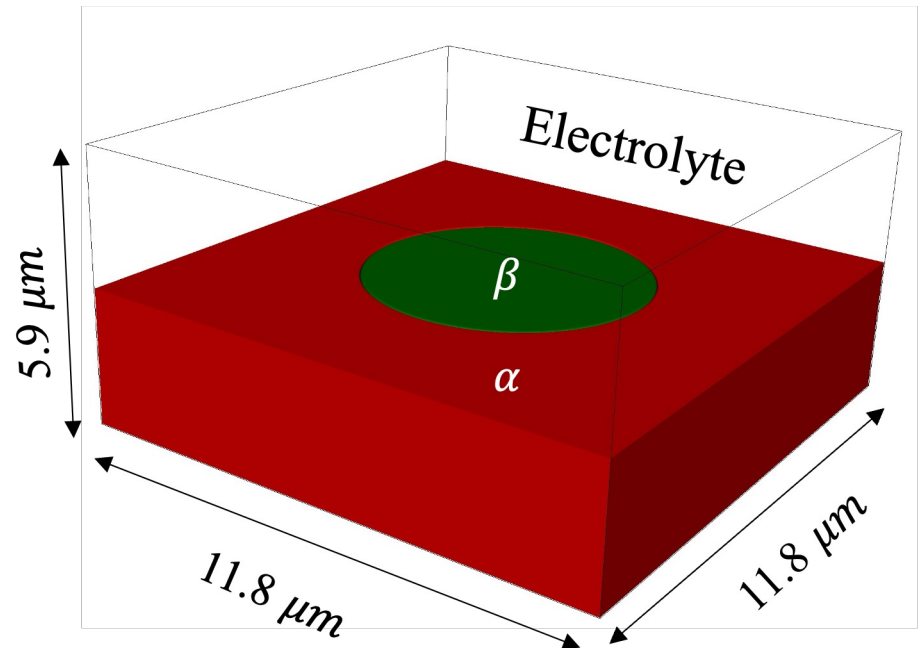
Simulation Setup

Effects of microstructures, as well as material properties were examined

2D System



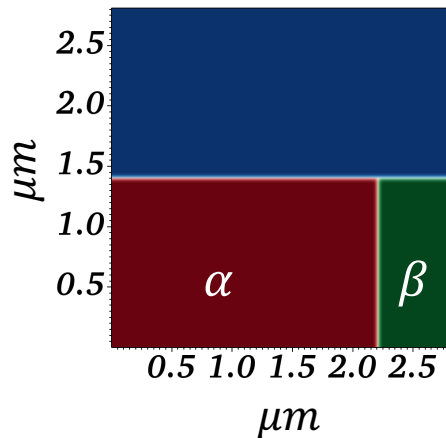
3D System



Goel et al., MRS Communications, 2022; Goel et al., J. ECS, 2023.

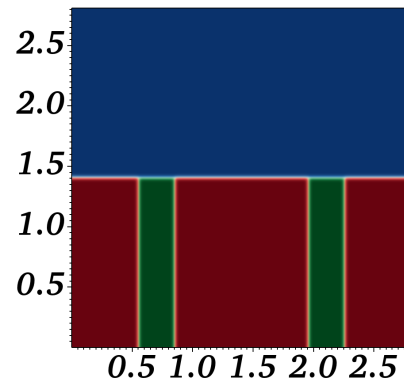
Effect of lamellae on the microgalvanic corrosion rate – 4 different 2D microstructures, 21% β

Case - 1



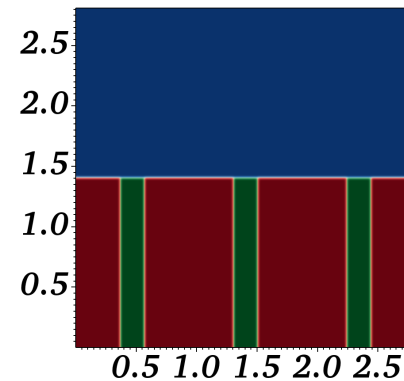
- Wide lamellar

Case - 2



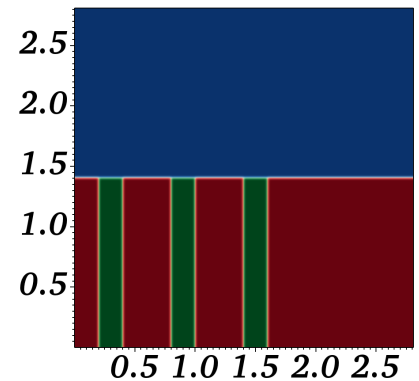
- Medium lamellar

Case - 3



- Narrow lamellar

Case - 4

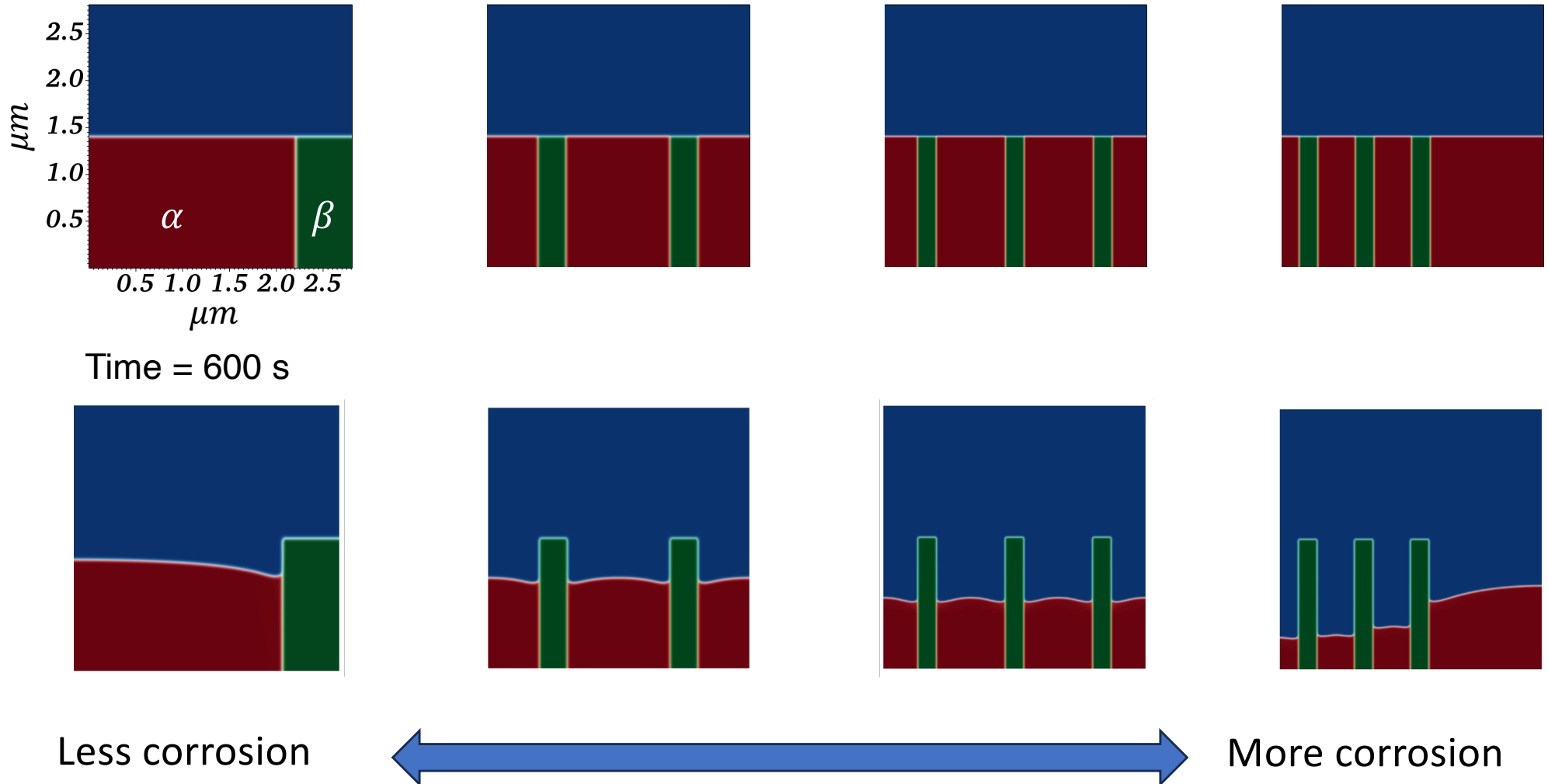


- Lamellar region next to a larger α region

Goel et al., J. ECS, 2023.

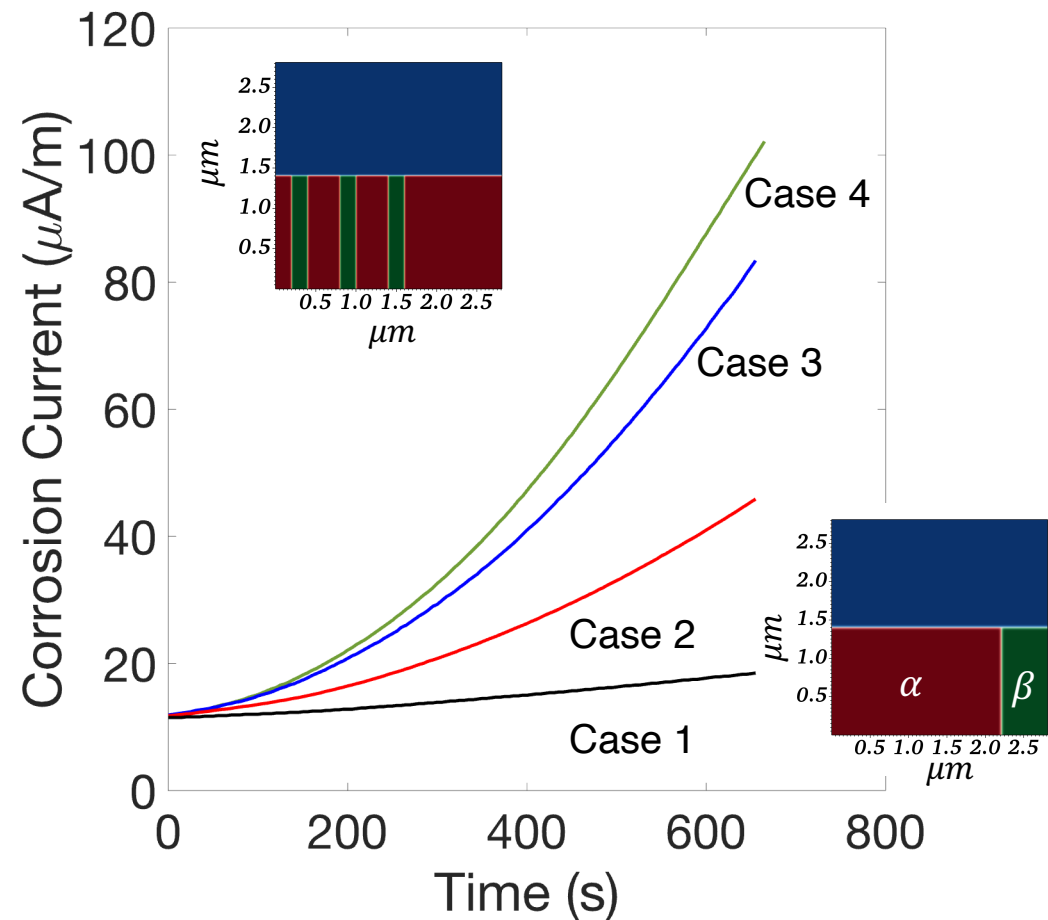
Effect of lamellae on the microgalvanic corrosion rate – 4 different 2D microstructures, 21% β

Goel et al., J. ECS, 2023.



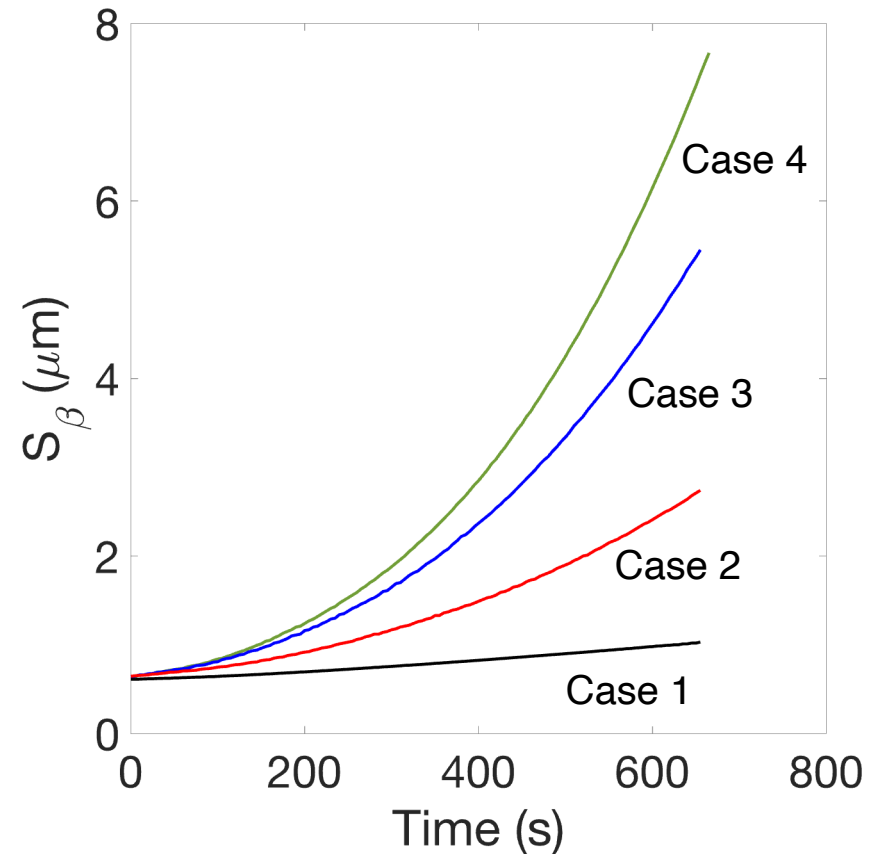
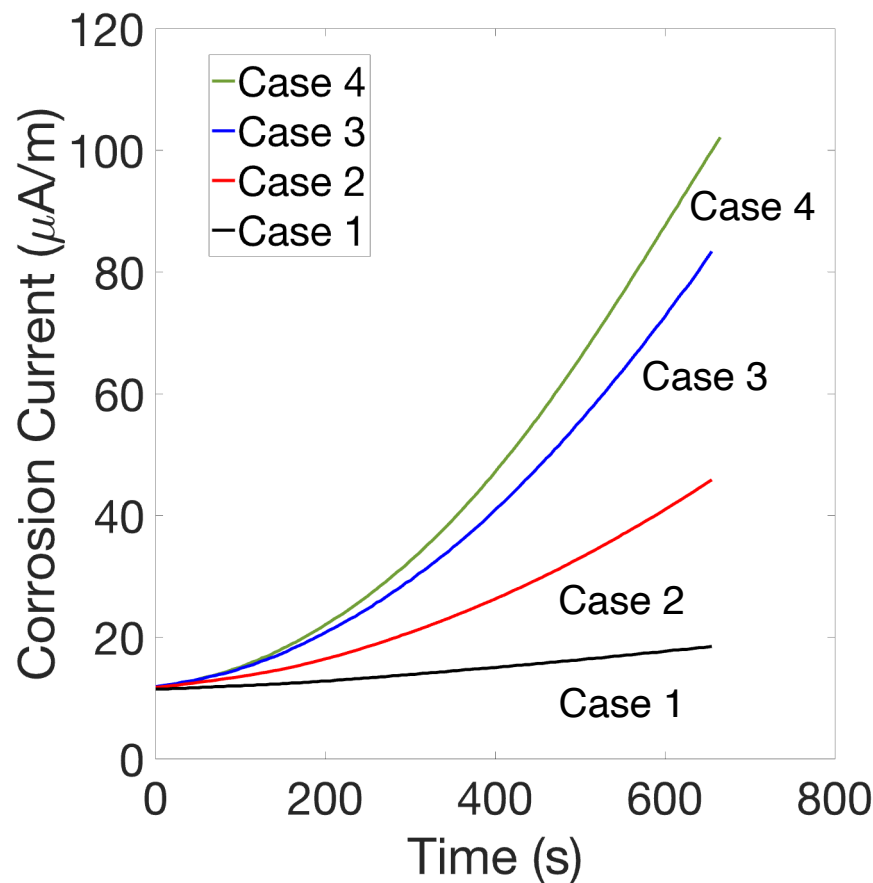
Presence of the lamellar region is detrimental to the corrosion resistance

- Quantification via corrosion current
- In all cases, the rate increases
- Finer lamellar structure show the largest corrosion rate
- Why?



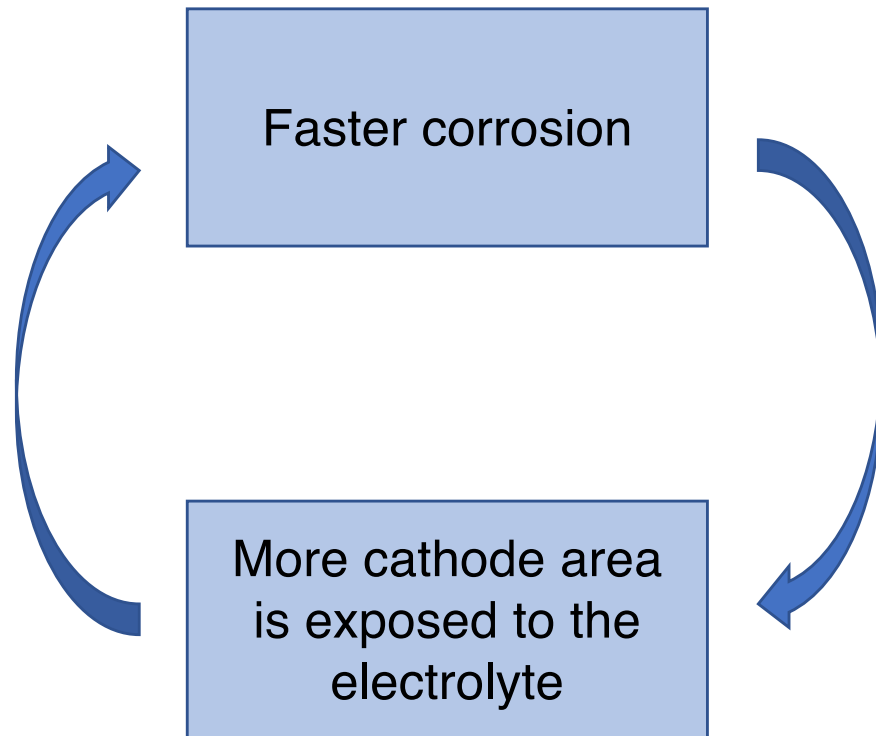
Goel et al., J. ECS, 2023.

Because it increases the cathode area exposed to the electrolyte with the progression of corrosion



Goel et al., J. ECS, 2023.

And thereby establishes a positive feedback loop



Also, the results highlight that it is NOT the volume of the cathodic component, but **the area that matters.**

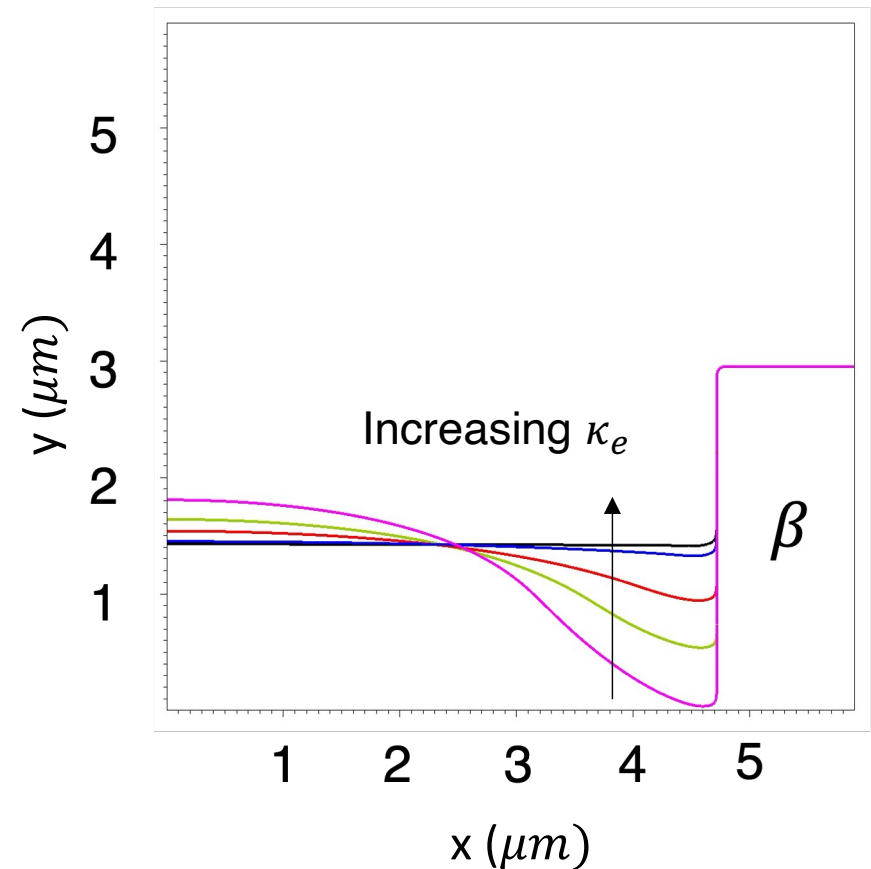
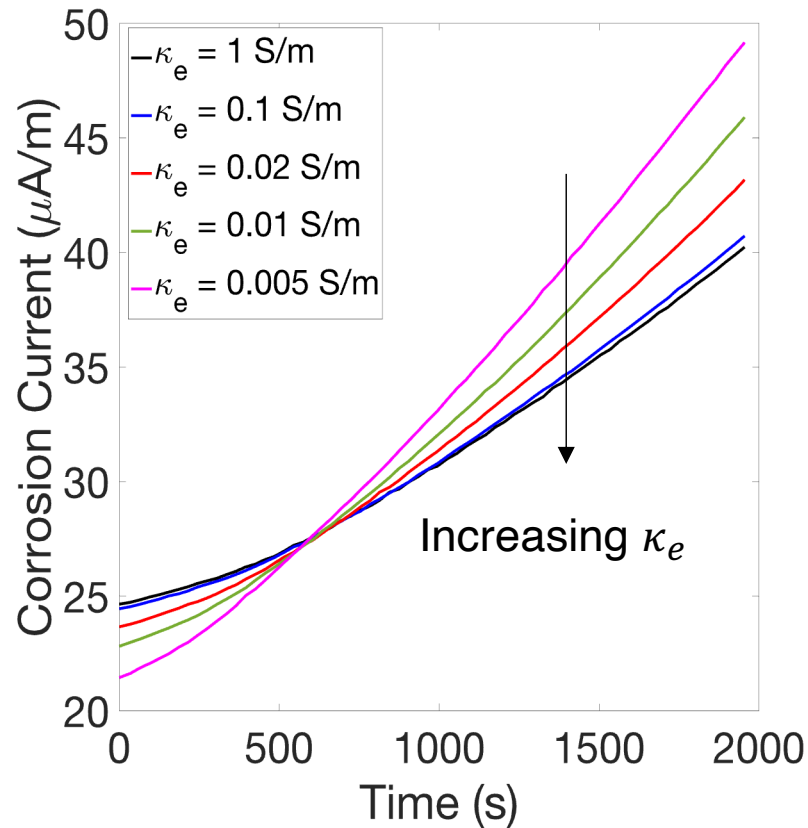
Goel et al., J. ECS, 2023.

High ionic conductivity improves the corrosion performance at later times due to the improved homogeneity of corrosion

Goel et al., J. ECS, 2023.

κ_e : the ionic conductivity of the electrolyte

Interface location
 $t = 2825$ s



Low κ_e initially has a lower rate of corrosion, but it then accelerates!

Wagner Length to Predicts the Nonuniformity in Corrosion

$$W_{\alpha} = \kappa_e \frac{\partial \eta_{\alpha}}{\partial i_{rxn,\alpha}}$$

Wagner et al., J. Electrochem. Soc., 98, 116 (1951)

- $W_{\alpha} \gg L_{\alpha}$ – Uniform corrosion
- $W_{\alpha} \ll L_{\alpha}$ – Nonuniform corrosion

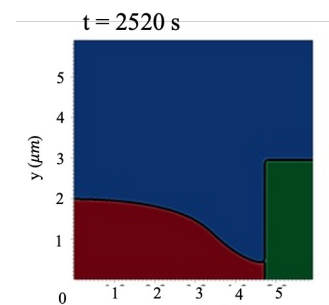
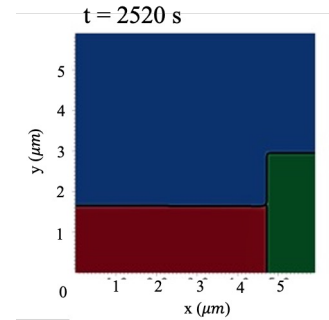
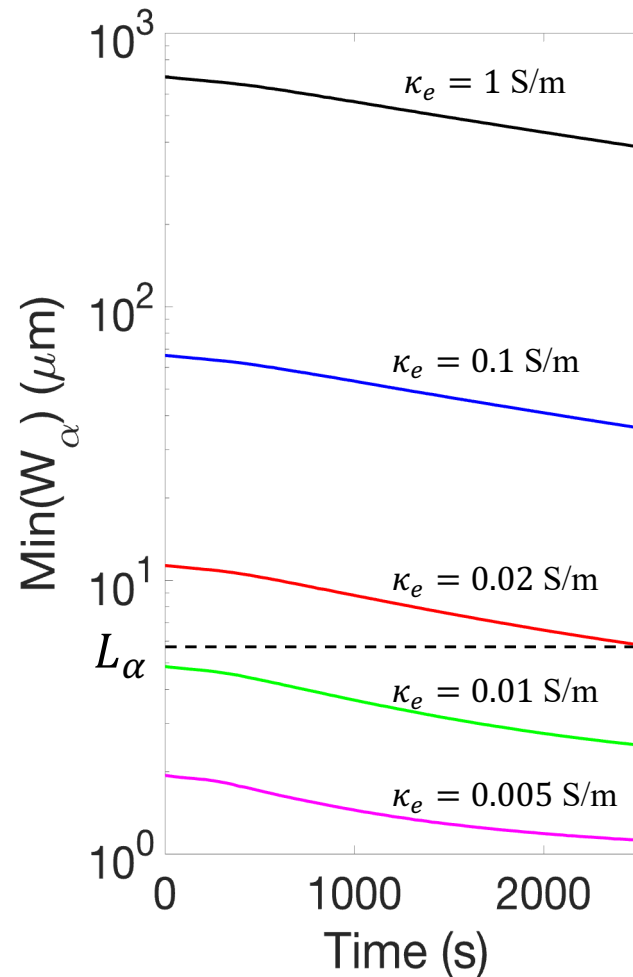
Affected by the material properties and microstructure

Effect of κ_e on the Wagner length

$W_\alpha \gg L_\alpha$ – Uniform corrosion



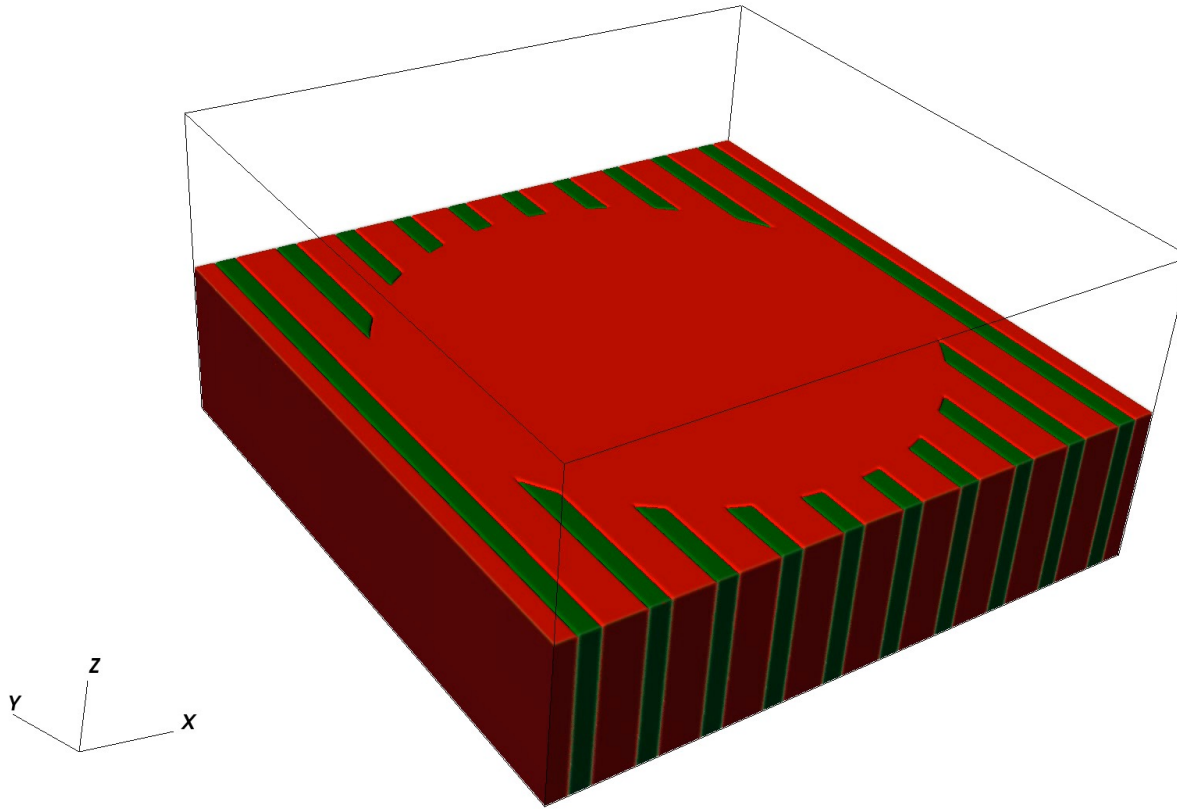
$W_\alpha \ll L_\alpha$ – Nonuniform corrosion



Goel et al., J. ECS, 2023.

Similar behavior is also observed in 3D

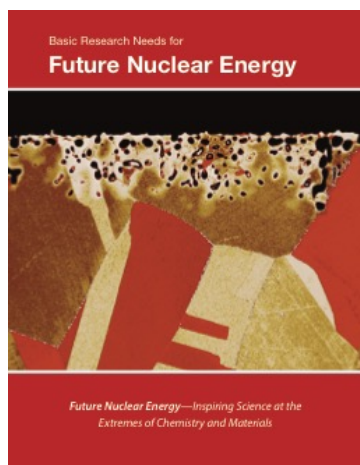
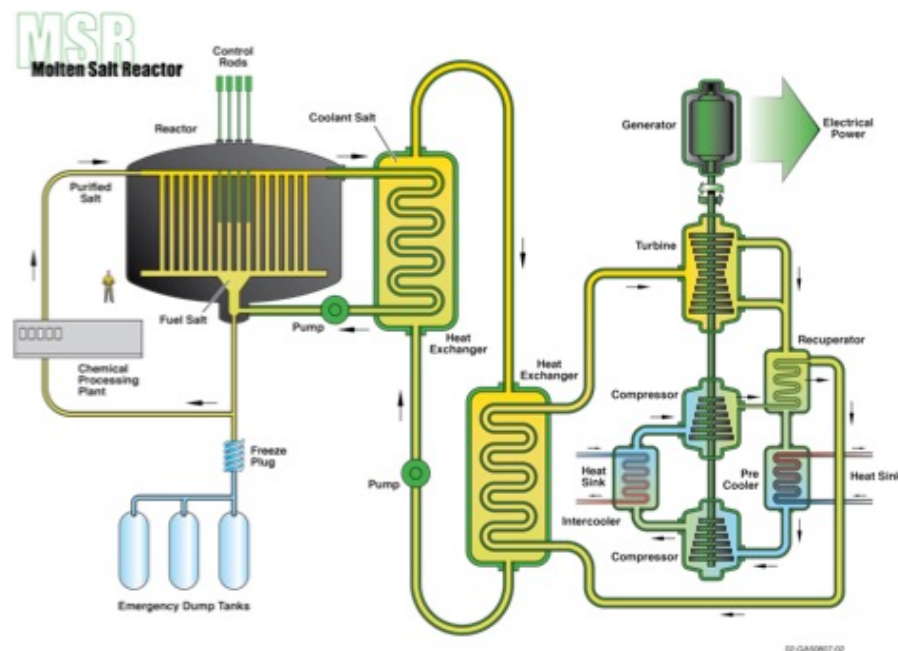
DB: solution-0000000.pvtu
Cycle: 0 Time:0



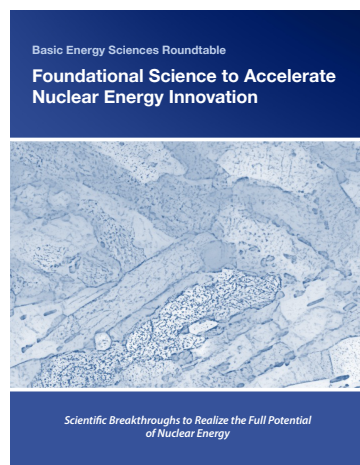
Goel et al., J. ECS, 2023.

Motivation for the MSEE EFRC: Molten Salt Reactors

- Leading candidates for next-generation nuclear reactors;
- Potential game-changing technology;
- Cost-competitive, safe, and more sustainable commercial nuclear power option.



2017 BES Workshop on
Basic Research Needs
for Future Nuclear Energy



2022 BES Roundtable on
Foundational Science to
Accelerate Nuclear Energy Innovation

Development of new MSR concepts requires fundamental understanding of, and development of predictive models for:

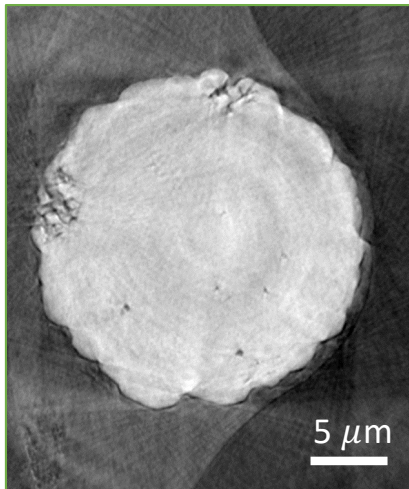
- the physics and chemistry of molten salts
- interactions with solutes (actinides, fission products, corrosion products) and radiation
- their interactions with, and degradation of, reactor materials.

Morphology in Ni-20Cr at 600°C vs 800°C

Liu et al. *Nat Commun* **12**, 3441 (2021)

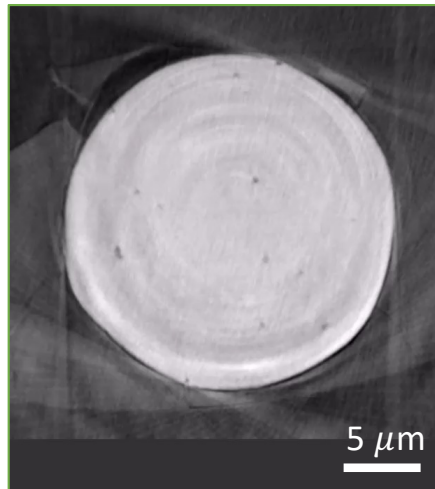
Liu et al. *ACS Appl. Mater. Interfaces*, **15**, 13772–13782 (2023)

600 °C

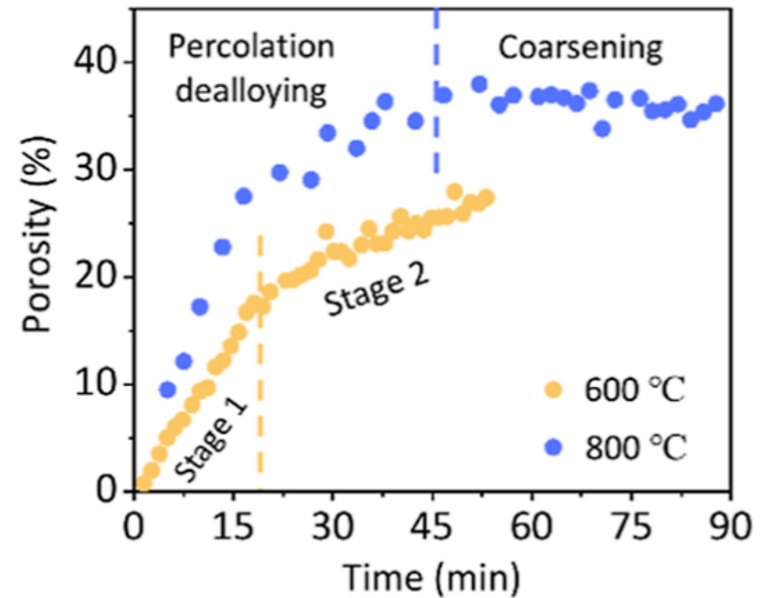


Intergranular Corrosion

800 °C



Percolation Dealloying

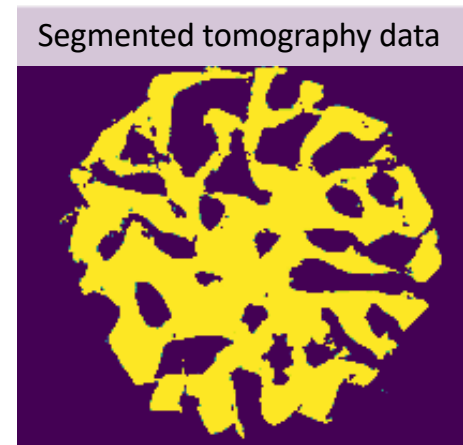
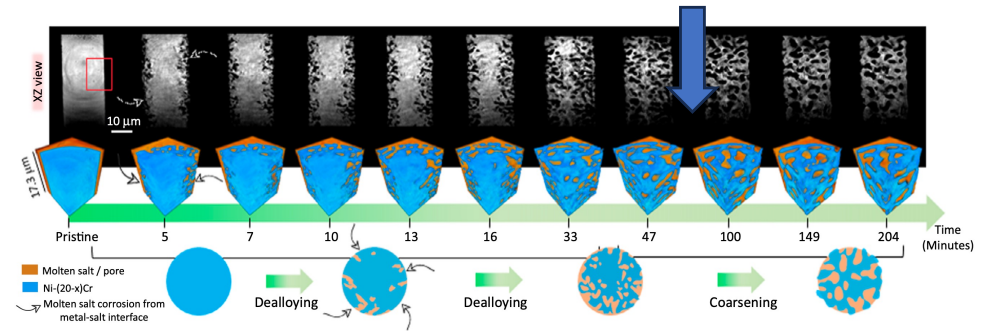


- Ni-20Cr wire in MgCl_2 -KCl salt
- Several mechanisms affect morphological evolution
 - Surface corrosion
 - Intergranular corrosion
 - Percolation dealloying
 - Surface diffusion

- Use the coarsening regime data to identify the dominant transport mechanism
- Simulate the corrosion regime with a parameterized model (ongoing)

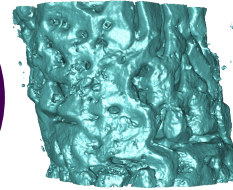
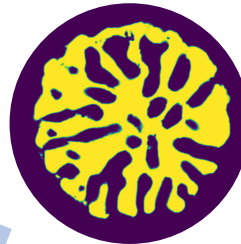
3D Coarsening Simulations

1. Initial condition from X-ray nanotomography experiment at the beginning of the coarsening stage
2. Smooth tomography data
3. Coarsen via...
 - Bulk diffusion through solid
 - Bulk diffusion through liquid
 - Surface diffusion

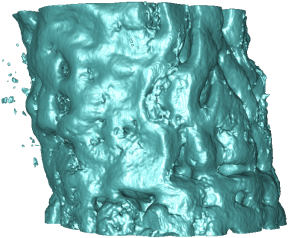


Morphological Evolution

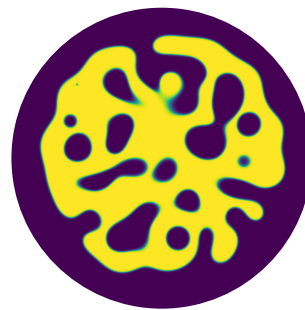
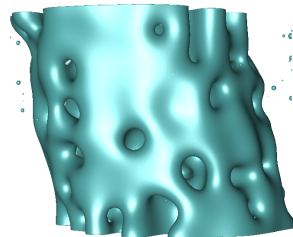
Experimental x-ray nanotomography,
initial condition, 65 mins



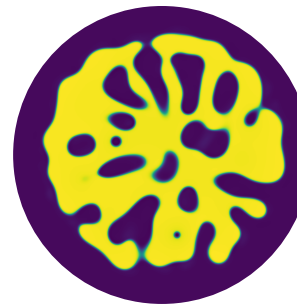
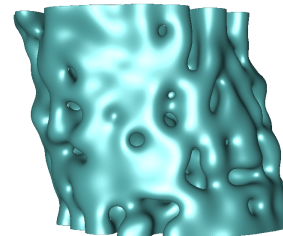
Experimental x-ray
nanotomography, 128 min



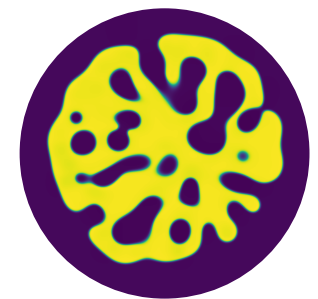
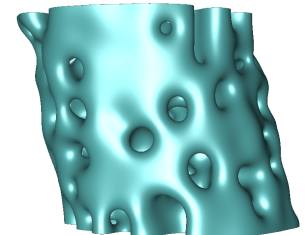
Simulation; surface diffusion,
 $t=969,700$



Simulation; solid bulk
diffusion, $t=105,700$



Simulation; liquid bulk
diffusion, $t=319,700$



COLLEGE OF ENGINEERING
MATERIALS SCIENCE & ENGINEERING
UNIVERSITY OF MICHIGAN



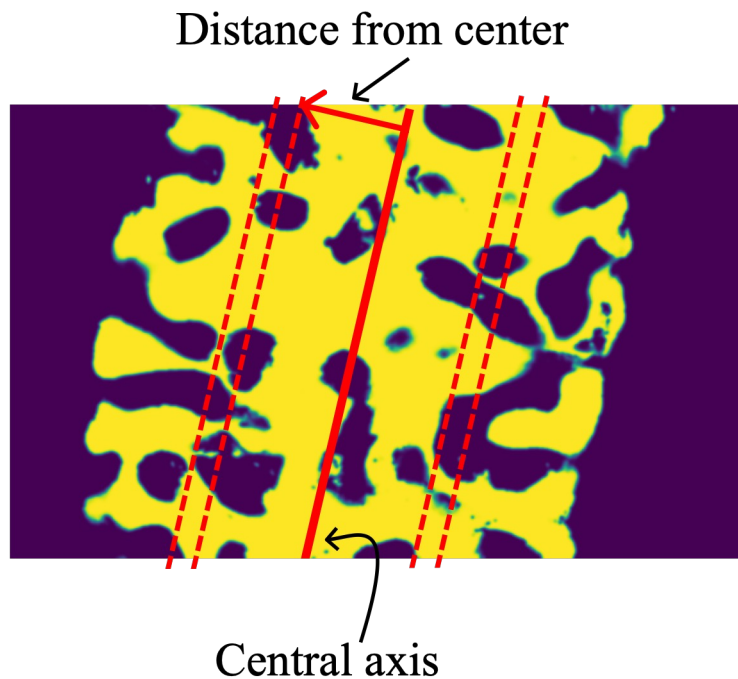
U.S. DEPARTMENT OF
ENERGY



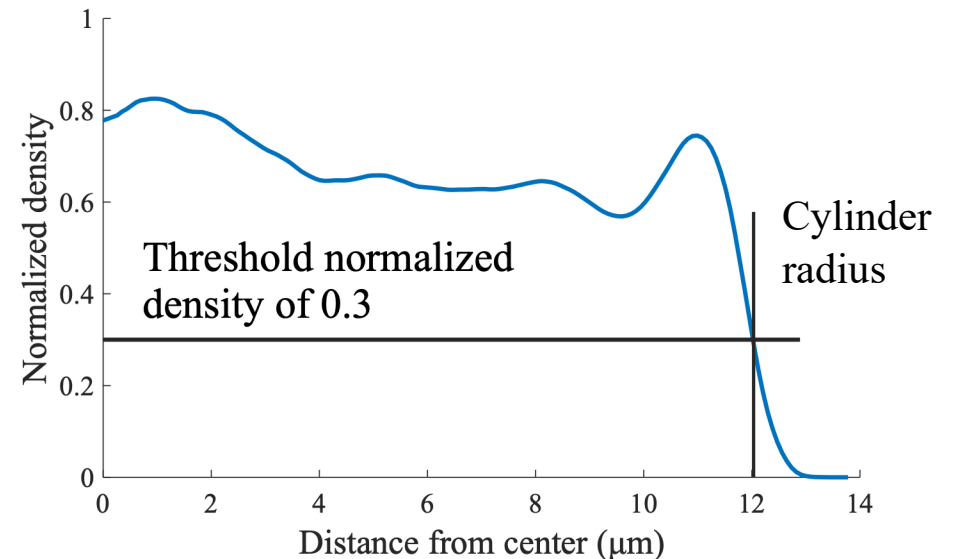
MSEE
molten salts in extreme environments



Quantifying Morphological Evolution: Radial Density Functions



Comparison is not trivial due to drift and noise in the experimental data

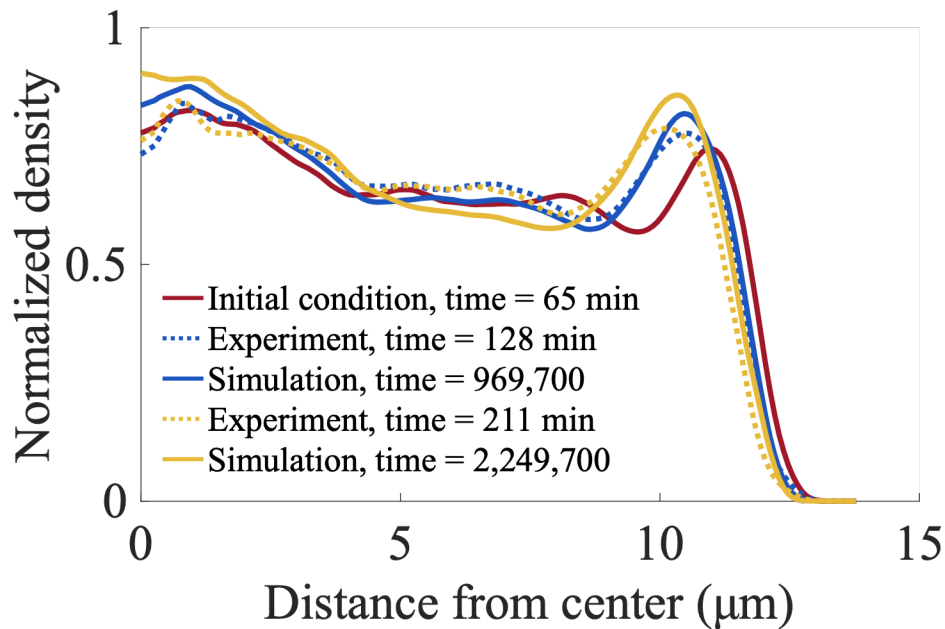


Note the schematics are in 2D, but the actual analyses are in 3D!

Matching the Timescales: Comparing Simulated and Experimental Morphologies

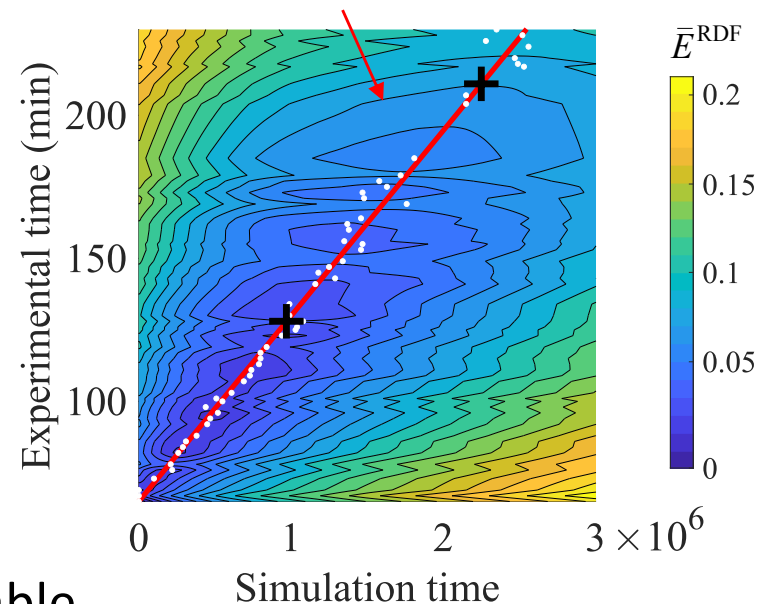
Example:

Surface Diffusion



Relative error between
experimental and simulated
radial density functions

$$t_{\text{exp}} = 6.48 \times 10^{-5} \text{ min } t_{\text{sim}} + 65 \text{ min}$$



Key Result: The comparison alone was not able to rule out bulk diffusion or surface diffusion.

Extracted Time Scaling Constant Can Be Used to Infer Diffusivities

	Cylinder radius	RDF	Best match from the literature
Surface diffusion (m^4/s)	1.80×10^{-28}	1.51×10^{-28}	1.69×10^{-29}
Solid bulk diffusion (m^3/s)	7.72×10^{-23}	7.50×10^{-23}	9.40×10^{-27}
Liquid bulk diffusion (m^3/s)	3.63×10^{-22}	2.26×10^{-22}	1.38×10^{-34}

Bulk diffusion

$$\frac{\gamma \Omega x_{\infty}}{k_B T} D = \frac{\ell^3}{30 \tau}$$

literature simulation

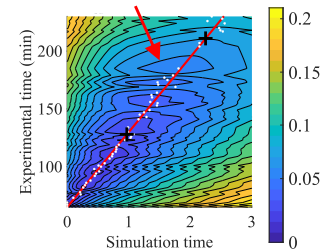
Surface diffusion

$$\frac{\gamma \Omega}{k_B T} D_s = \frac{\ell^4}{6 \tau}$$

literature simulation

ℓ is set by the spatial resolution of the simulation

τ is the slope of this line \bar{E}^{RDF}



Literature values can be found in Hendrix et al. *Acta Mater.* 297 (2025) 121299

Key Result: Surface diffusion is most likely the dominant mechanism, unless dealloying injects a large number of vacancies into the bulk.

Modeling Corrosion in Molten Salt

Experimentally observed mechanisms

- Surface corrosion
- Intergranular corrosion (enhanced corrosion on grain boundaries)
- Dealloying (involves bulk diffusion)

Other possible processes

- Grain boundary diffusion
- Grain growth
- Stress effect/cracking

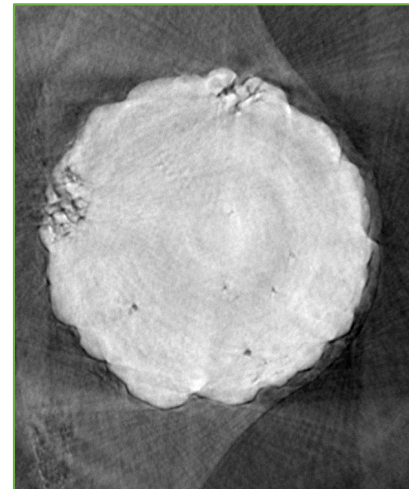
Modeling Corrosion in Molten Salt

Experimentally observed mechanisms

- ✓ Surface corrosion
- ✓ Intergranular corrosion (enhanced corrosion on grain boundaries)
 - Dealloying (involves bulk diffusion)

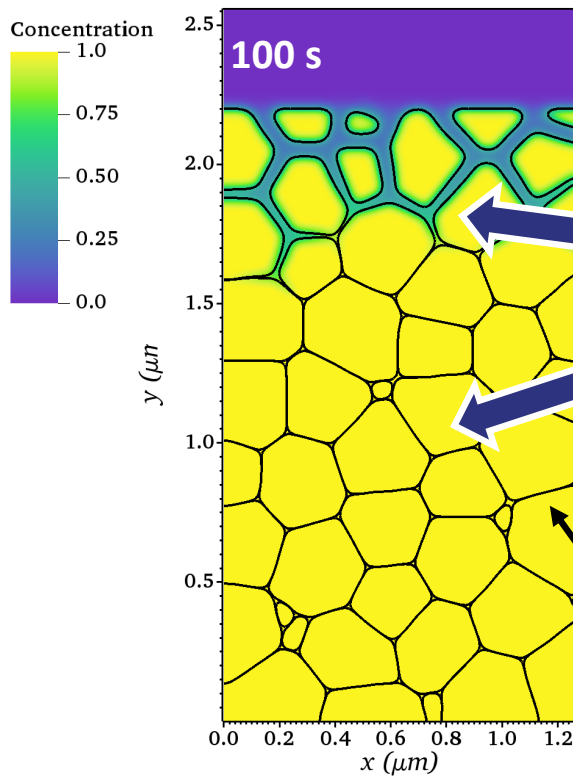
Other possible processes

- Grain boundary diffusion
- ✓ Grain growth
- Stress effect/cracking



Intergranular Corrosion in a Pure Metal

Grain interfaces controlled by Allen-Cahn equation



$$\frac{\partial \eta_i}{\partial t} = -L \frac{\delta \mathcal{F}}{\delta \eta_i}$$

- Consider case of 100% Cr ($c_{\text{Cr}} = \sum_i \eta_i$)
- Assume well-stirred and well-supported limit for the electrolyte

Lines mark $\eta_i = 0.5$ contours or grain boundaries

- The initial condition is a 2D slice from a structure generated in Dream3D

Groeber and Jackson. *Integr Mater Manuf Innov* **3**, 56–72 (2014)

Intergranular Corrosion in a Pure Metal

Metal/electrolyte interface evolution controlled by

$$\underbrace{\frac{\partial \psi_1}{\partial t} = \nabla \cdot \left[M(\psi_1) \frac{\delta \mathcal{F}}{\delta \psi_1} \right]}_{\text{Cahn-Hilliard evolution}} - \underbrace{v |\nabla \psi_1|}_{\text{Interfacial velocity}}$$

Cahn-Hilliard evolution

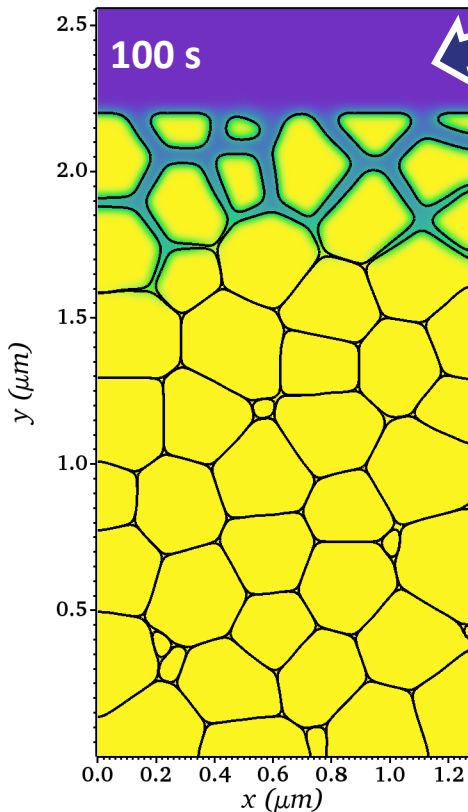
Interfacial velocity

$$v = - \left(\frac{V_M}{z_M F} \right) i_{\text{rxn}}$$

Reaction current governed by Butler-Volmer equation

$$i_{\text{rxn}} = \sum_{j=1}^N \left[i_{\text{corr},j} \exp \left(\frac{z_M (1 - \beta) F}{RT} \eta \right) \left(\xi_j + 16\alpha \sum_{k>j}^N \xi_j^2 \xi_k^2 \right) \right]$$

α controls the enhancement of GB corrosion

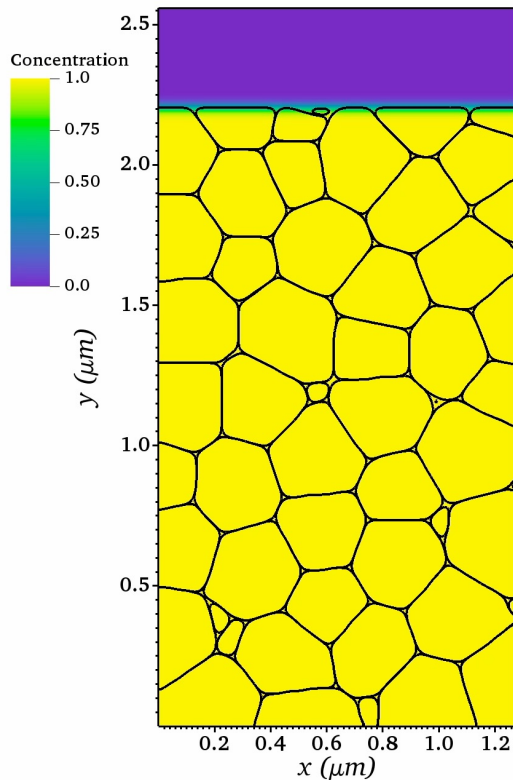


Intergranular Corrosion in a Pure Metal

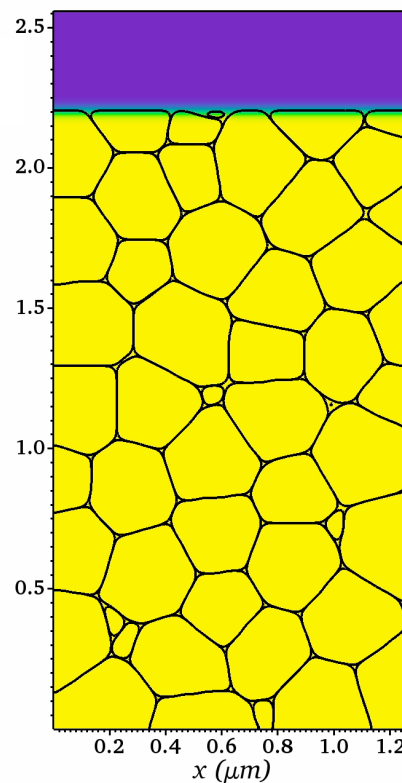
Surface corrosion only

With GB corrosion

$\alpha = 0$



$\alpha = 5$



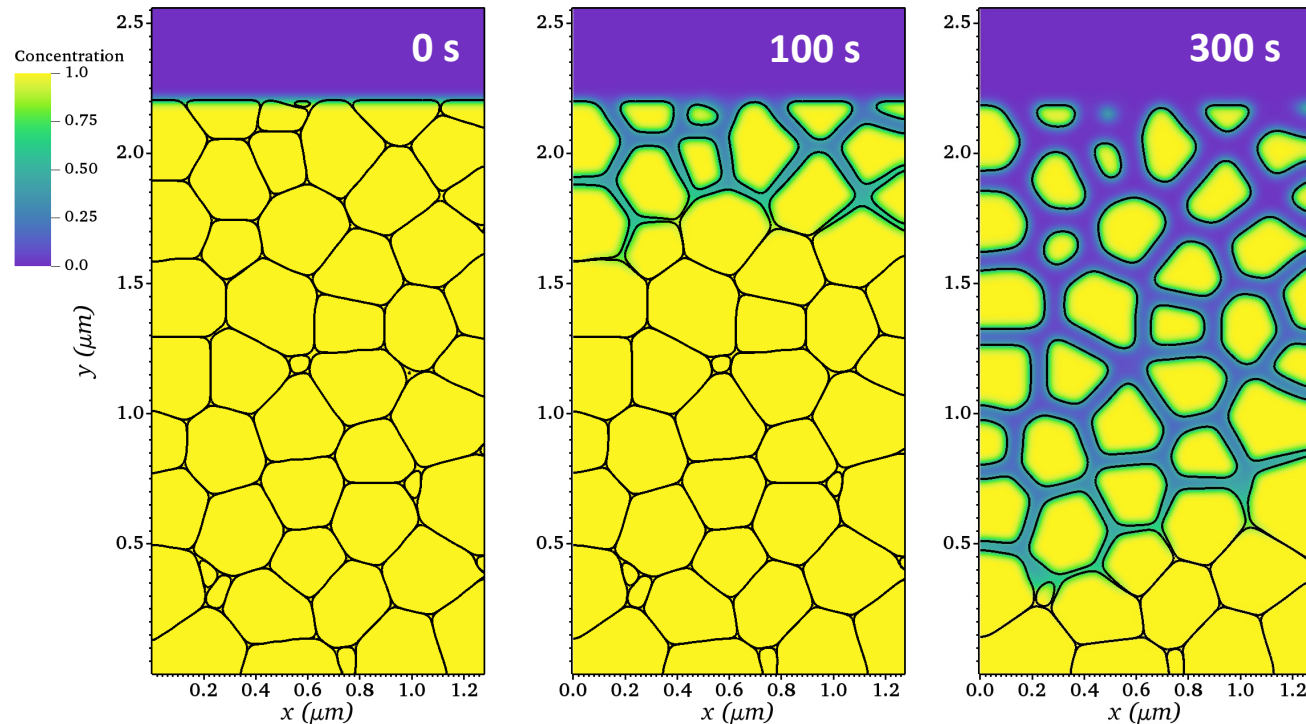
Left:

- Surface recedes nearly uniformly.
- Grain growth is observed

Right:

- Rapid corrosion along grain boundaries leads to potential detachment of grain remnants

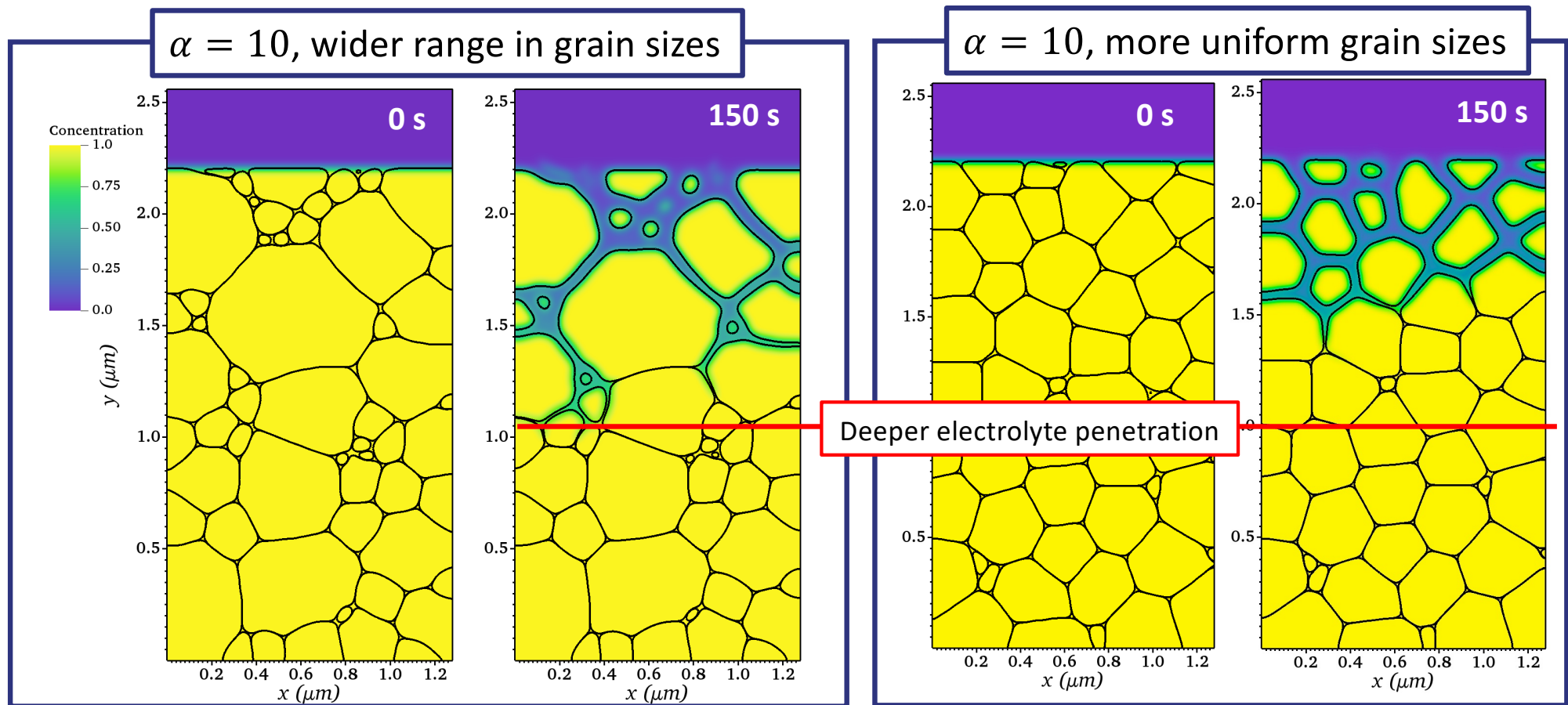
Intergranular Corrosion in a Pure Metal



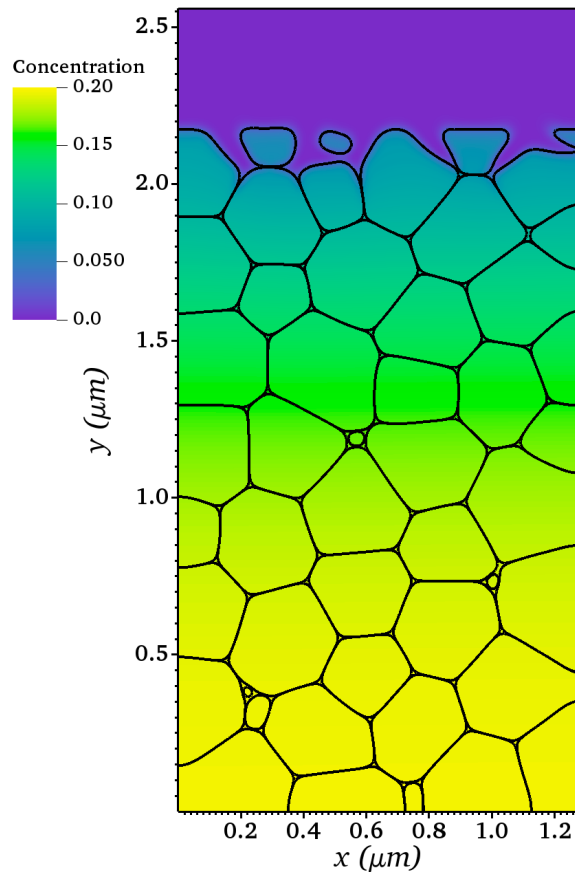
- We demonstrated that intergranular corrosion can be modeled along with grain growth
- While the detachment is exaggerated in 2D, nanoparticle formation is experimentally observed

Effect of Microstructure on Corrosion Behavior

Wider grain size distribution leads to faster corrosion because of the dissolution of small grains and larger ion diffusion path!



Intergranular Corrosion in an Alloy



We track the Cr concentration in the alloy using the smoothed boundary method (SBM):

$$\frac{\partial c_{\text{Cr}}}{\partial t} = \frac{1}{\psi_s} \nabla \cdot (\psi_s D \nabla c_{\text{Cr}}) - \frac{|\nabla \psi_s|}{\psi_s} \left(\frac{i_{\text{rxn}}}{zF} \right)$$

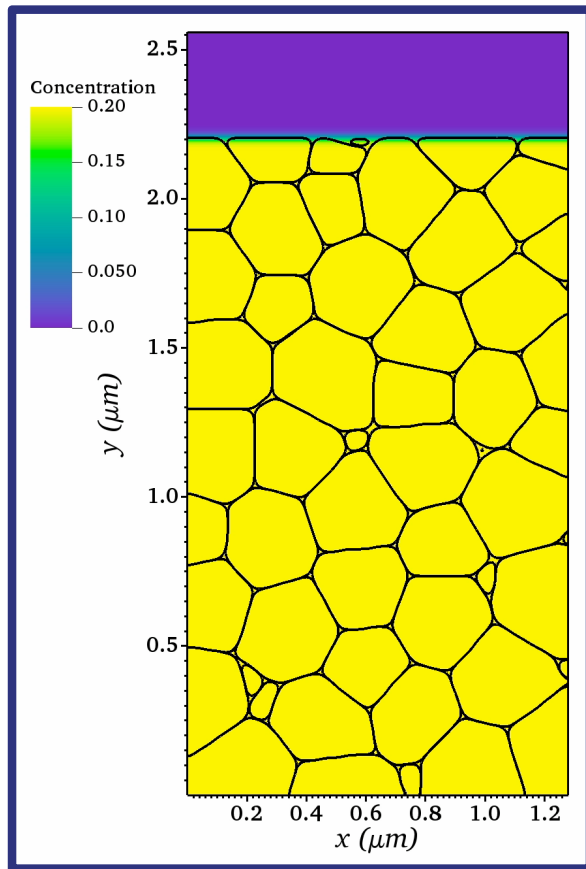
$\psi_s = 1 - \psi_l$ is the domain parameter for the solid phase
Restricts concentration of Cr to the solid phase

We calculate the overpotential from the chemical potential of Cr in molten chloride salt

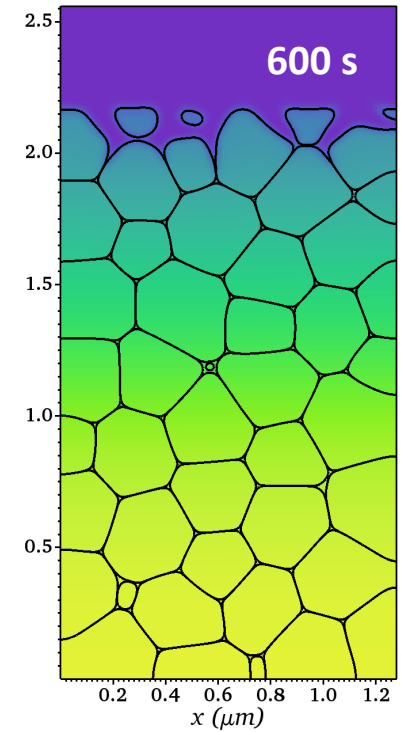
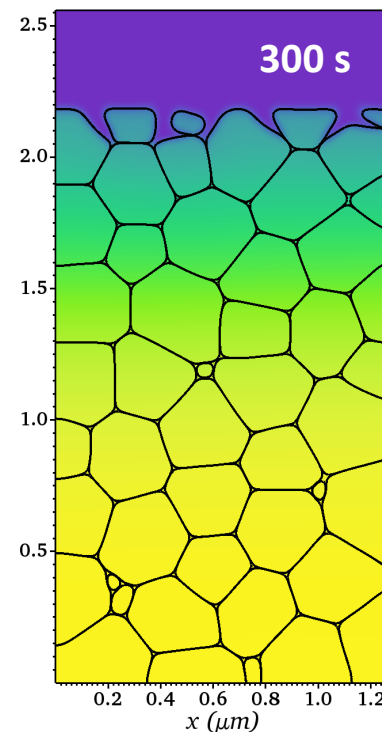
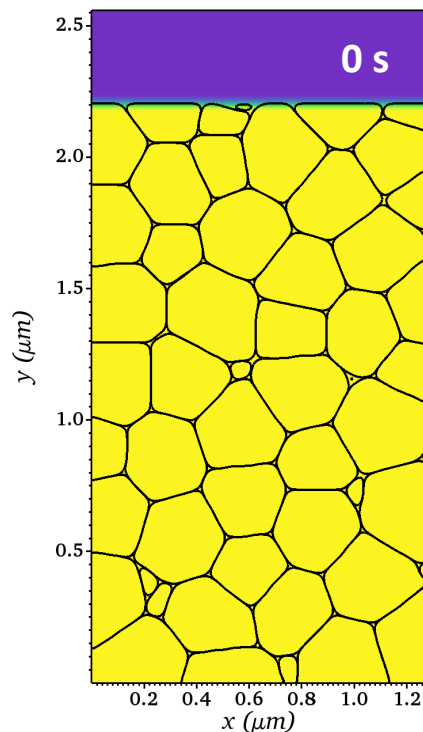
$$i_{\text{rxn}} = \sum_{j=1}^N \left[i_{\text{corr},j} \exp \left(\frac{z_M(1-\beta)F}{RT} (\mu_{\text{Cr}} - \mu_{\text{Cr,eq}}) \right) \left(\xi_j + 16\alpha \sum_{k>j}^N \xi_j^2 \xi_k^2 \right) \right]$$

Intergranular Corrosion in an Alloy

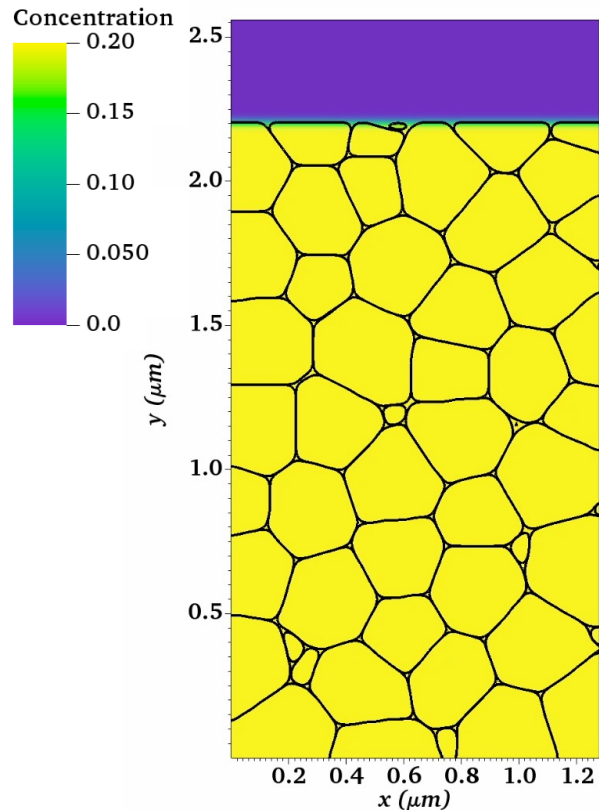
Simply changing the model to a two-component system did not yield a result similar to the experiment! – What's missing?



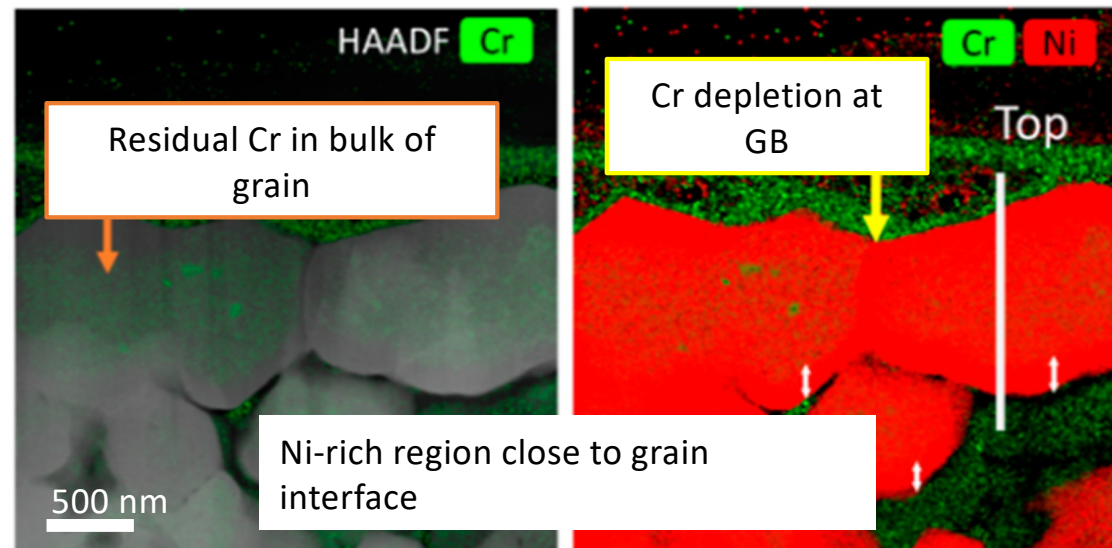
$$\alpha = 10$$



Enhanced Diffusivity at the Grain Boundary



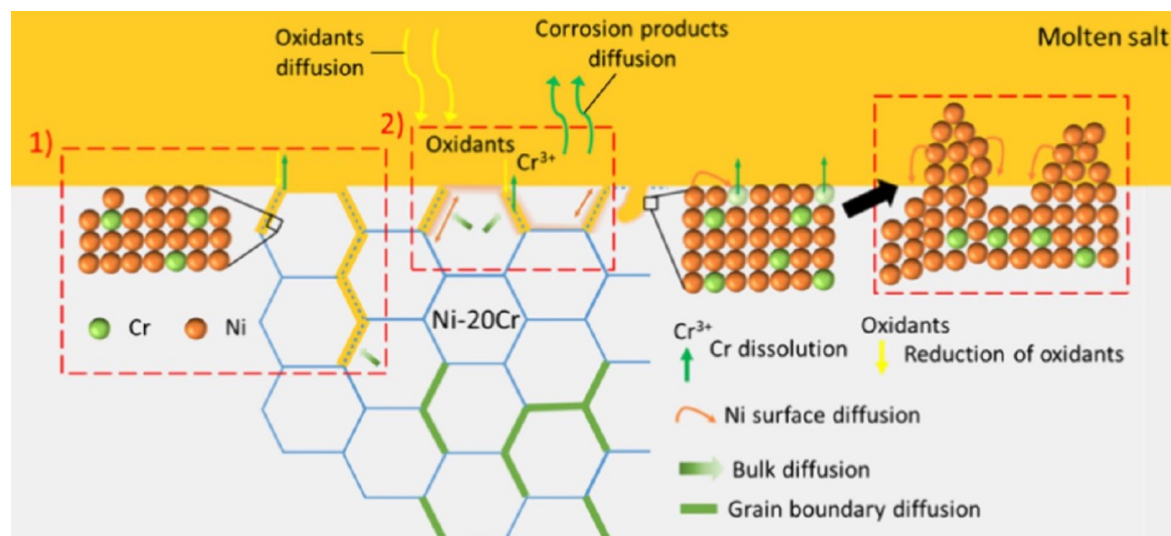
$$D = \sum_{j=1}^N \left[\xi_j D_{\text{bulk}} + 16 D_{\text{GB}} \sum_{k>j}^N \xi_j^2 \xi_k^2 \right]$$



EDS analysis of Ni-20Cr sample after intergranular corrosion

Liu et al. *ACS Appl. Mater. Interfaces*, **15**, 13772–13782 (2023)

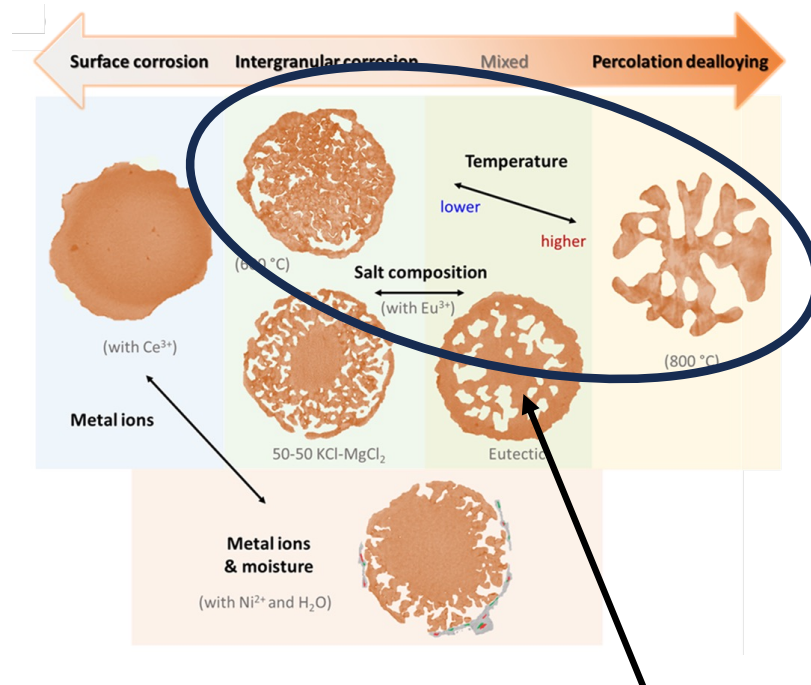
Working Towards the Morphological “Phase Diagrams”



- Challenge: Parameterization of the model
- We need to link electronic structure/atomistic simulations to model parameters!



Liu et al. *ACS Appl. Mater. Interfaces*, **16** (34) 45606–45618 (2024)
 Liu et al. *ACS Appl. Mater. Interfaces*, **15**, 13772–13782 (2023)



How does this transition occur?

Take-Aways

- We developed an open-source software application in PRISMS-PF for the materials science community to simulate corrosion.
- Presented two example applications:
 - Corrosion in magnesium alloys
 - Corrosion in molten salt informed by experiments
- Microstructural effects:
 - The surface area of the cathodic material has a strong effect on how corrosion is accelerated
 - Grain size distribution has an important consequence on the grain boundary corrosion
 - Grain boundary diffusion may be important in molten salt corrosion
 - Electrochemical processes can amplify the stochastic nature of the microstructure; **how can we take this into account on a coarse-grained model?**

Thank you!